JPRS L/9513

29 January 1981

USSR Report

PHYSICS AND MATHEMATICS

(FOUO 1/81)

FBIS FOREIGN BROADCAST INFORMATION SERVICE

NOTE

JPRS publications contain information primarily from foreign newspapers, periodicals and books, but also from news agency transmissions and broadcasts. Materials from foreign-language sources are translated; those from English-language sources are transcribed or reprinted, with the original phrasing and other characteristics retained.

Headlines, editorial reports, and material enclosed in brackets [] are supplied by JPRS. Processing indicators such as [Text] or [Excerpt] in the first line of each item, or following the last line of a brief, indicate how the original information was processed. Where no processing indicator is given, the information was summarized or extracted.

Unfamiliar names rendered phonetically or transliterated are enclosed in parentheses. Words or names preceded by a question mark and enclosed in parentheses were not clear in the original but have been supplied as appropriate in context. Other unattributed parenthetical notes within the body of an item originate with the source. Times within items are as given by source.

The contents of this publication in no way represent the policies, views or attitudes of the U.S. Government.

APPROVED FOR RELEASE: 2007/02/08: CIA-RDP82-00850R000300070048-9

JPRS L/9513

29 January 1981

USSR REPORT

PHYSICS AND MATHEMATICS

(FOUO 1/81)

CONTENTS

LASERS AND MASERS

UDC 621.373.826.038.823

PHOTOLYSIS LASERS FOR CONTROLLED NUCLEAR FUSION

Moscow IZVESTIYA AKADEMII NAUK SSSR: SERIYA FIZICHESKAYA in Russian Vol 44, No 10, Oct 80 pp 2002-2017

[Article by S. B. Kormer]

[Text] Introduction

A typical feature of photolysis lasers proposed in 1961 by the authors of Ref. 1 is a rather wide band of absorption of pumping radiation ($\sim 10^3 cm^{-1}$) similar to the absorption band of solid-state lasers in combination with a narrow luminescence line of 10^{-2}-10^{-1} cm^{-1}. This makes it possible to achieve high gains and a low lasing threshold.

Lasing in this type of laser was first attained [Ref. 2, 3] on molecules of CH_3I and CF_3I ($RI + h\nu \rightarrow R + I^*$). Emission wavelength is $\lambda = 1.315$ μm. An energy of 1-5 mJ was achieved. A rather cumbersome flash photolysis iodine laser was developed in 1966 [Ref. 4], giving a laser energy of 65 J for 1.5 ms.

Stimulated emission was reported in a Q-switched iodine laser in Ref. 5, although it was not until 1971 that interest arose in such lasers for research in the field of nuclear fusion, when Ref. 6 was published, the first of a large series of papers on work at the Max-Planck Institute in Garching. In these papers, on the basis of research results, the iodine laser was offered as one of the possible competitors of neodymium and CO_2 lasers for controlled nuclear fusion. Possibilities of using iodine lasers for these purposes were explored by Soviet [Ref. 7, 8], U. S. [Ref. 9, 10] and British [Ref. 11] scientists*.

Outside of the Soviet Union, the best results have been attained at Max-Planck Institute. For example it was reported in Ref. 12 that an energy of 300 J was attained in a pulse with duration of $(1\text{-}3)\cdot 10^{-9}$ s with efficiency of ~ 0.1% with respect to the energy stored in a capacitive accumulator. In the brief paper of Ref. 13 mention is made of attainment of 500 J at $\tau_{1/2} = 0.5\cdot 10^{-9}$ s. In the USSR the maximum energies that have been attained in the period up to publication of the present report have been ~ 300 J in 10^{-9} s at an efficiency of 0.1% [Ref. 14] and 500 J in $1.5\cdot 10^{-9}$ s at the same efficiency [Ref. 15]. However, these figures are far from exhausting the capabilities of iodine lasers. For example, specialists at the Max-Planck Institute are of the opinion that there is a real possibility of making

*Here and below we cite only the first papers by the different authors.

iodine lasers with pulse energy of 10-100 kJ at a duration of 0.1 ns and with a pulse recurrence rate of 100 Hz.

Among the advantages of iodine lasers, mention should be made of the following.

1. Capability of fairly uniform circulation of large cross sections of working fluid, and in this way giving large energies in a single beam, which enables selection of the optimum number of active elements of a laser facility for given energy.

2. Capability of regulating the width of the luminescence line of the working transition by adding a buffer gas. This enables optimization of gain of the laser medium and duration of the lasing pulse. At atmospheric pressure it is possible to amplify pulses with $\tau \geqslant 40$-100 ps [Ref. 17].

3. Comparatively long lifetime of the excited iodine and comparatively short pumping duration, which reduces the intensity of superluminescence.

4. Comparatively minor optical inhomogeneities of the working medium and capability of achieving relatively small divergence of emission.

5. Fewer limitations associated with radiation strength of the working medium (self-focusing and the like).

These advantages of the iodine laser put it on the same level [Ref. 18, 19] with more perfected neodymium lasers and CO_2 gas lasers.

In this paper we give our principal attention to a survey of the results realized in our own research [Ref. 8, 15, 20-29].

1. Working fluids and processes. Estimation of output energy of amplifiers

The most estensively used working fluids for iodine lasers are the organic iodides CF_3I and C_3F_7I. The absorption band of these compounds has a maximum at $\lambda_{max} \approx 270$ nm with half-amplitude width of about 35 nm. The absorption cross section at the maximum is $(6\text{-}8)\cdot10^{-19}$ cm^2, which corresponds to an absorption coefficient $\alpha \approx 2\cdot10^{-2}$ (torr·cm)$^{-1}$. The relatively low coefficient of absorption enables fairly uniform circulation through working volumes with a large aperture.

Upon absorption of an ultraviolet quantum, the working fluid dissociates into a radical and an electronically excited iodine atom:

$$C_3F_7I+h\nu_{\text{л}} \rightarrow C_3F_7+I^*(^2P_{1/2}).$$

Studies have shown that the quantum yield in this case is close to unity. The laser transition is between levels $^2P_{1/2}$ and $^2P_{3/2}$ of the iodine atom, which have a hyperfine structure [Ref. 30, 31]. The resultant laser emission wavelength is 1.315 μm.

One of the distinguishing features of the given active media is the capability of varying the amplification cross section σ over a rather wide range by adding buffer gases such as CO_2, SF_6, Ar and others. When this is done, the cross section σ

decreases with increasing partial pressure of both the working fluid itself and the buffer gases [Ref. 17]. This increases the latitude of development of iodine lasers since it gives a means of attaining relatively low weak-signal gains at high specific densities of the stored and output energies.

The expected energy parameters of each of the amplifiers with assumption of uniform population inversion over its cross section and lengthwise can be determined from an expression [Ref. 32] that describes the amplification process:

$$\varepsilon_{вых}=\varepsilon_{нас}\ln\left[K_0\left(\exp\frac{\varepsilon_{вх}}{\varepsilon_{нас}}-1\right)+1\right], \quad (1)$$

$$K_0=\exp\sigma_{34}NL, \quad (2)$$

$$\varepsilon_{нас}=\frac{h\nu}{\sigma_{34}\left(1+\frac{g_в}{g_н}\right)}=\frac{24}{31}\frac{h\nu}{\sigma_{34}}. \quad (3)$$

Here $\varepsilon_{ВХ}$ and $\varepsilon_{ВЫХ}$ are respectively the density of the input and output energies of the amplifier; K_0 is the weak-signal gain; σ_{34} is the amplification cross section on transition $F_В = 3 \to F_Н = 4$; N is the initial population of excited particles on the sublevel with quantum number $F_В = 3$; L is the length of the amplifier; $\varepsilon_{НАС}$ is the saturation energy of the working transition $F_В = 3 \to F_Н = 4$; $g_В$ and $g_Н$ are the statistical weights of the upper and lower sublevels participating in the transition.

For the sake of simplicity, relations (2) and (3) are given for the most frequently encountered case where the lasing transition is between the sublevel with quantum number $F_В = 3$ of level $^2P_{1/2}$ and sublevel $F_Н = 4$ of level $^2P_{3/2}$. It was also taken into consideration that in accordance with Ref. 31 the upper sublevels in the case of interest to us $\tau \lesssim 10^{-9}$ s do not have time to relax relative to one another, while the sublevels of level $^2P_{3/2}$ do have time. Then $g_В = 7$, $g_Н = 24$.

In the limiting case when $\varepsilon_{ВХ} \gg \varepsilon_{ВЫХ}$, (1) implies

$$\varepsilon_{вых.\ пред}=\varepsilon_{нас}\ln K_0+\varepsilon_{вх}. \quad (4)$$

From (2)-(4) we get

$$\varepsilon_{вых.\ пр}-\varepsilon_{вх}=\frac{24}{31}h\nu NL=\frac{14}{31}\varepsilon_{зап.\ полн}, \quad (5)$$

where

$$\varepsilon_{зап.\ полн}=h\nu N_0 L, \quad N_0=\frac{\Sigma g_в}{g_в=3}N=\frac{12}{7}N.$$

The total stored energy $\varepsilon_{ЗАП.\ ПОЛН}$ on level $^2P_{1/2}$, which must be known for calculating the output energy from (5), can be found from the free lasing energy $\varepsilon_{СВ.\ ГЕН}$. In the approximation of fairly rapid "cleaning" of the lower lasing

level ($^2P_{1/2}$) as a result of recombination of an unexcited iodine atom with a radical [Ref. 17]

$$\varepsilon_{\text{зап. пол}} = \varepsilon_{\text{св. ген}} + \varepsilon_{\text{пор}}, \tag{6}$$

where $\varepsilon_{\text{пор}}$ is the threshold energy.

In designing an amplifier that operates in the monopulse mode, when the input signal is applied at the instant of the first zero of the pumping current to prevent the influence that the uncompensated magnetic field of the pumping sources has on the spectrum of the hyperfine structure of atomic iodine, it is necessary to take consideration only of the energy that has been stored up to this instant:

$$\varepsilon_{\text{зап моно}} = \gamma(\varepsilon_{\text{св. ген}} + \varepsilon_{\text{пор}}), \tag{7}$$

where γ is the fraction of the stored energy on level $^2P_{1/2}$ by the instant of arrival of the monopulse.

Experimental studies of the time dependence of lasing power have shown that the first half-period of the current of the final amplifiers contains about 70% of the energy stored in the accumulator. Therefore the value of $\varepsilon_{\text{зап. моно}}$ from (7) must be used in (5).

If we know the stored energy on the working sublevel, we can find the amplification cross section that ensures a given weak-signal gain. The necessary value of σ_{34} is attained by varying the buffer gas and its pressure [Ref. 17]:

$$\frac{1}{\sigma_{34}} = \beta_0 - \sum_i \varepsilon_i P_i, \tag{8}$$

where β_0 is the Doppler component of luminescence line broadening, β_i is the coefficient of collisional broadening of the different gases at pressure $[P_i]$.

The permissible values of K_0 in amplifiers depend on a number of factors such as the optical decoupling mechanisms that are used, the presence of vacuum selectors, parasitic reflectors and the like. Experience has shown that in order to avoid self-excitation of amplifiers, K_0 must be kept to the order of 10^2 or less, particularly in the final amplifiers.

In Section 5 on the basis of the relations given above, estimates of the output energy of amplifiers are made and compared with experimental results.

2. Concerning the degree of uniformity of pumping and the optical homogeneity of the working medium in an iodine laser

In extensive use for pumping iodine lasers are both flashlamps [Ref. 4, 6, 8, 33, 34] and an open electric discharge in the working mixture. The authors of Ref. 7, 35, 36 used an exploding wire to initiate discharge in a gas. We utilized reusable large-aperture discharge pumping sources with traveling discharge proposed and developed by the authors of [Ref. 15] in our amplifiers.

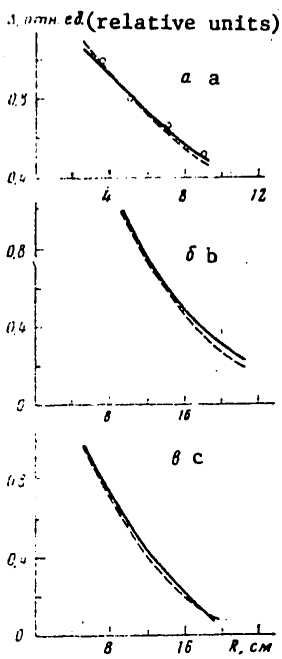

Fig. 1

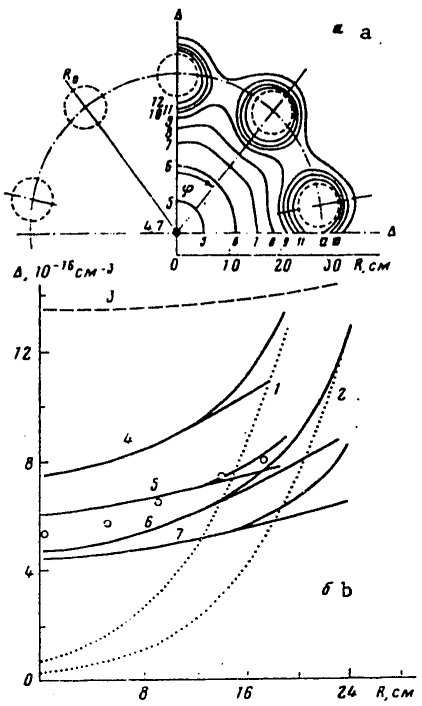

Fig. 2

Fig. 1. Distribution of inversion with respect to radius of the cell (broken lines show the calculation, solid lines show the experiment): a--lamp source ($p_{C_3F_7I}$ = 5 mm Hg); b--electric discharge source ($p_{C_3F_7I}$ = 5 mm Hg); c--exploding wire ($p_{C_3F_7I}$ = 7.5 mm Hg)

Fig. 2. a--Isolines of population inversion; b--distribution of inversion with respect to radius of the cell with pumping by one or more sources. Calculation: dotted lines--1 source; solid lines--9 sources; broken line--40 sources; 1, 2, 3, 4, 6--$p_{C_3F_7I}$ = 4.5 mm Hg; 5, 7--3 mm Hg. Experiment: points--9 sources, p_0=3 mm Hg

Fig. 1 shows the results of a study of uniformity of circulation through the working volume of a large-aperture laser when a lamp source or electric discharge source [Ref. 15, 37] is placed on the axis of the cell. The experimental value of the dependence of inversion Δ on radius R is determined either directly or from the distribution of free lasing over the end face. The behavior of $\Delta(R)$ observed with pumping by different sources is determined not only by the absorption of quanta in the working medium, but also by purely geometric reduction of the density of quanta with increasing radius.

The nonuniformity of inversion distribution can be reduced by reducing the partial pressure of the working mixture, and also by increasing the number of pumping

sources in the working volume. The latter approach is especially necessary for making large-aperture amplifiers (see Fig. 2a). Optimization of the number of sources and the radius of their configuration was done by a special program of two-dimensional calculation of photodissociation. This program accounts for the time dependence of the brightness temperature of the source $T_{br}(t)$ and the actual profile of the absorption band of the working fluid. The program is also suitable for calculation of electrodischarge pumping sources with expanding emission surface.

The results of some calculations are shown in Fig. 2b, where the radial distribution of inversion is shown with variation of the radius of source placement, the number of sources and the partial pressure of the working fluid. We can see that if a single source is placed in a cell with $R_0 = 20$ cm (curves 1 and 2), the inversion differential at $p_0 = 4.5$ mm Hg of C_3F_7I will exceed 15. On the other hand, if about 40 sources or more are placed on the outer surface of the cell, inversion will be nearly uniform over the entire cross section (curve 3). When the number of sources is reduced to 9 (curves 4, 5, 6 and 7), the difference in inversion increases. For example if the sources are placed at $R_0 = 22.5$ cm, this difference reaches a factor of 1.5-2 at $p_0 = 4.5$ mm Hg, and a factor of 1.3-1.5 at $p_0 = 3$ mm Hg (curves 4 and 5).

As we can see from the figure, the experimentally found distribution of inversion in free lasing runs agrees fairly well with calculated results (curve 5).

The degree of inversion nonuniformity with respect to angle with nine sources can be seen from Fig. 2a, which gives the pattern of isolines of population inversion at $p_0(C_3F_7I) = 4.5$ mm Hg and $R_0 = 27.5$ cm. Angular nonuniformity shows up at $R_0 > 15$ cm and increases as the sources are approached. The maximum nonuniformity of inversion density with respect to angle for the given arrangement is 30%.

On the basis of experiments and the results of theoretical optimization we have now decided that in future research we will use nine reusable traveling-discharge sources placed at $R_0 = 22.5$ cm. The optical inhomogeneity of the active medium has been studied experimentally for these conditions. Similar studies have also been done for amplifiers with flashlamp pumping in which the active medium was contained in quartz cells. (A more detailed description of the amplifiers will be given below.)

Measurements were made in the driven mode of amplifier operation close to the pumping sources, where optical inhomogeneities should be maximum. The amplifier medium to be studied was placed in one of the arms of a Michelson interferometer. The studies were done on a wavelength of 0.63 μm, analogously to the way that this had been done previously [Ref. 22, 24-27, 36] (see also Ref. 38). The gradient of the index of refraction and its dependence on distance r from the pumping source were determined from the profile of the index of refraction of the medium found at the instant of zero current.

The resultant curves of $\text{grad}\, n = f(r)$ for the working media of three amplifiers are shown in Fig. 3. We can see that in all amplifiers grad n decreases with increasing distance from the pumping source. The width of the zone of optical inhomogeneities is 1.5-2 cm. Increasing the pressure of the working fluid (C_3F_7I) in the amplifiers leads to an increase in grad n. At the same time, the absolute values of grad n are such as to enable attainment of good divergence. For example,

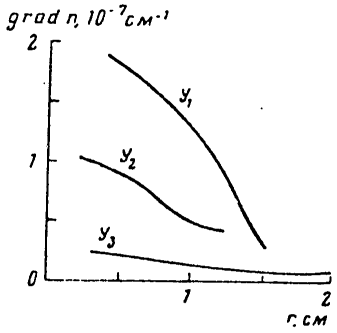

Fig. 3. Change in the gradient of the index of refraction with respect to the radius of the cell (r is distance from the pumping source): Y_1--30 mm Hg C_3F_7I + 440 mm Hg SF_6; Y_2--22 mm Hg C_3F_7I + 370 mm Hg SF_6; Y_3--3.7 mm Hg C_3F_7I + 150 mm Hg CO_2 + 440 mm Hg Ar

if a plane wave is sent to the input of the first amplifier, the divergence at the output of the third amplifier due to the found values of the gradient of the refractive index should not exceed $\theta_{E/2} \approx 0.5 \cdot 10^{-4}$ radian.

3. Optical decoupling mechanisms and radiation contrast

One of the problems in developing facilities for laser-driven nuclear fusion is attainment of high radiation contrast* (10^7-10^8). For this purpose, multistage amplification systems use special means that forestall self-excitation of the amplifiers, and specifically such optical decoupling devices as Pockels cells, Kerr cells and phototropic dyes. Here an examination will be made of methods that we have suggested and studied [Ref. 8, 20, 21, 29].

To ensure adequate contrast at the output of the entire system, we must consider the fact that the weak-signal gain in each amplifier is of the order of 10^2, while the strong-signal gain (see relation (1)) is about 10-15. This means that the radiation contrast in each stage will deteriorate by a factor of about 10, and the role of interstage decoupling is not only to compensate for deterioration of the contrast, but to improve it. The careful selection of the parameters of the individual amplifiers should serve this same purpose.

A very important parameter of interstage decoupling that determines the feasibility of application of a given mechanism in a given design for preventing self-excitation of the amplifiers and increasing radiation contrast is the ratio of transmission of the main radiation pulse T_{strong} to transmission of the weak signal (background) $\kappa = T_{strong}/T_{weak}$. Since T_{strong} determines the losses in the decoupling mechanism, the ratio must be close to 100%.

To solve this problem, the authors of Ref. 8, 20 proposed and developed a passive iodine shutter. This device is a saturable absorber that operates on the resonant transition $2P_{3/2} \rightarrow 2P_{1/2}$ of the iodine atom. It has been experimentally shown [Ref. 8, 20, 39] that the weak-signal absorption factor in such a shutter reaches 10^3, whereas monopulse transmission is ~80% for a sufficiently intense incident signal.

The intensity dependence of transmission experimentally found [Ref. 20] for iodine laser emission with pulse duration $\tau \approx 5 \cdot 10^{-6}$ s through the shutter at T = 1050°C with concentration of atomic iodine of $\sim 3.5 \cdot 10^{17}$ cm^{-3} and molecular iodine concentration of $\sim 10^{17}$ cm^{-3} is given in Fig. 4a together with the theoretical dependence $I/I_0 = f(I_0)$ found at a molecular iodine quenching constant of $1.8 \cdot 10^{-11}$ cm^3 s^{-1}. For effective laser operation it is necessary that the width of the absorption line

*Radiation contrast is defined as the ratio of the energy of radiation in a monopulse to the energy incident on the target before arrival of the pulse.

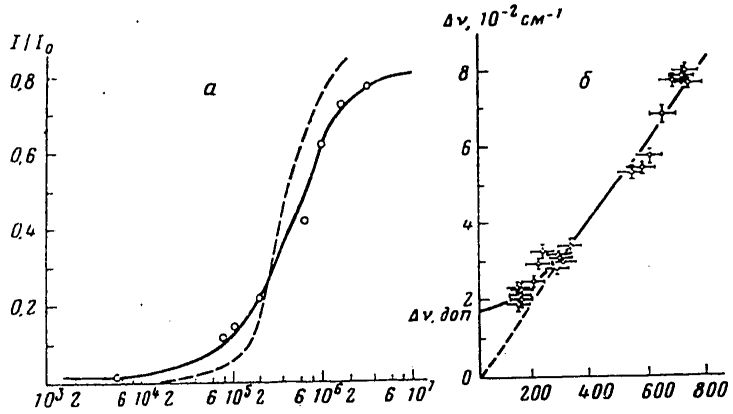

Fig. 4. a--Transmission of the iodine shutter as a function of intensity (T=1050°C; $N_1 = 3.5 \cdot 10^{17}$ cm^{-3}). Points and solid curve -- experiment, broken line -- theory. b--Absorption linewidth as a function of pressure in the cell ($\Delta\nu/\Delta p \approx 10^4$ $cm \cdot torr^{-1}$) (points show experimental data).

be close to that of the amplification line. When this is so, the absorption cross section is somewhat larger than the amplification cross section.

Results of investigations of the way that absorption linewidth depends on the total pressure in the cell are shown in Fig. 4b, from which we can see that as pressure increases beginning at about 300 mm Hg, the absorption linewidth increases in proportion to pressure with a widening constant of $\Delta\nu/\Delta p = 10^{-4}$ $cm \cdot torr^{-1}$. Knowing this dependence, we are able to choose the optimum parameters of the iodine shutter. However, there are serious difficulties involved in developing an iodine shutter with aperture greater than 100 mm that is capable of transmitting energy measured in the hundreds of joules. Therefore, we investigated the feasibility of using an optical decoupling mechanism based on thin metal coatings sputtered on glass substrates [Ref. 29]* that become transparent to light under the action of laser radiation due to the low degree of ionization of metal during vaporization.

Analysis of the thermophysical and optical properties of a number of metals has shown that bismuth meets the necessary requirements. Table 1 gives the results of an experimental study of the reduction in opacity of thin bismuth films with weak signal passage of from 0.15 to 10%.

For a film with $T_{weak} = 1\%$, strong signal transmission ranged from [illegible] to 75% with a change in the incident energy density from 0.7 to 2.1 J/cm^2 (Fig. [illegible]).

Variation of T_{weak} by two orders of magnitude (see Table 1) leads to a relatively small change in T_{strong}. Possibly two coatings may be best, each of which passes a weak signal with $T_{weak} = 10\%$ ($\Sigma T_{weak} = 1\%$, $T_{strong} = 80$-90%).

*Such films had been used previously [Ref. 40] to shorten pulse duration.

TABLE 1

T_{weak}, %	ε_{inc}, J/cm^2	ε_{trans}, J/cm^2	T_{strong}, %*	κ
0.15	1.7	0.88	52	345
0.25	1.9	1.22	63	250
1	1.5	1.13	70	70
2	1.5	1.2	80	40
5	1.26	1.1	87	17
10	0.26-0.4	0.23-0.38	90-95	9
2·10	0.26-0.4	0.12-0.36	80-90	80

*$T_{strong} = \varepsilon_{trans}/\varepsilon_{inc}$

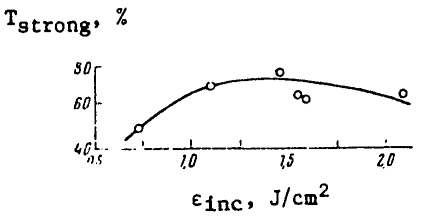

Fig. 5. Transmission of thin bismuth coatings ($T_{weak} \approx 1\%$)

Experimental values of $\kappa = T_{strong}/T_{weak}$ (Table 1) practically cover the working range of weak-signal gains of iodine amplifiers (50-500), which enables us to choose a monopulse amplification mode without deterioration of the radiation contrast obtained at the output of the master laser, and to prevent self-excitation of adjacent amplification stages. Such shutters with diameter of about 50 cm can handle laser beams with energy of a few kJ with fairly low losses of energy to reduction of opacity (~10-20%) and fairly high attenuation of the background signal (by a factor of the order of 10^2 or more). This method can also be used to prevent self-excitation of an amplifier due to reflection of emission from the target. Here it is sufficient to use a coating with $T_{weak} = 10\%$ to reduce the parasitic coefficient of reflection from the target by a factor of 100 with a double pass through the coating.

We also investigated the feasibility of using nonlinear phenomena like stimulated Mandelstam-Brillouin scattering (SMBS)* for interstage decoupling and obtaining high contrast [Ref. 21, 23, 28]. This possibility is determined by the threshold nature of onset of stimulated scattering. One arrangement for improving contrast and cutting off the preliminary pulse that may arise in the master laser is shown in Fig. 6.

For iodine lasers with a narrow luminescence band $\Delta\nu \approx 0.1$ cm^{-1} [Ref. 44], heavy compressed gases with a slow speed of sound (Xe, SF_6) can serve as a working fluid for SMBS; however, such media have a long relaxation time. As a result, the mode of excitation of SMBS becomes very unsteady.

*At present considerable attention is being given to the possibility of using the phenomenon of wavefront reversal [Ref. 41] for compensation of optical inhomogeneities [Ref. 42] and for guiding radiation to the targets [Ref. 28, 43] in laser-driven fusion facilities.

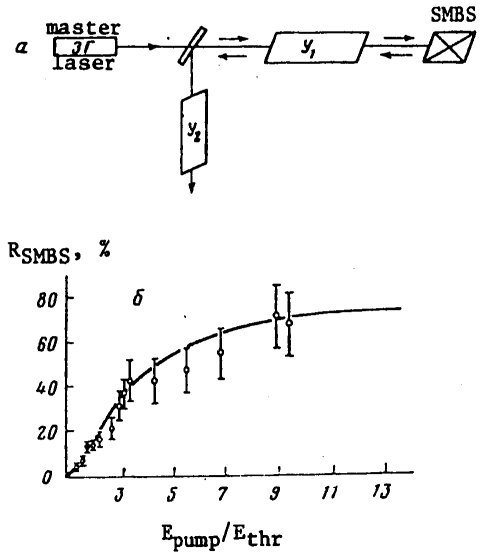

Fig. 6. a--Experimental setup; b--reflectivity of SMBS mirror as a function of excess over the threshold ($E_{thr} = 2.5$ J/cm^2). Points -- experiment; curve -- calculation

The possibility of getting any high values of the coefficients of reflection from SMBS mirrors (R_{SMBS}) under these conditions seemed problematic and required experimental studies, the results of which are shown in Fig. 6 in the form of a curve for R_{SMBS} as a function of excess of the pumping energy (E_{pump}) over the threshold energy (E_{thr}). The maximum coefficient of reflection $R_{SMBS} = 70\%$. A numerical study of the energy characteristics of the Stokes pulse in the case of SMBS for unsteady interaction as done in Ref. 23 in the plane-wave approximation showed good agreement with the experiment (curve on Fig. 6).

TABLE 2

Radiation contrast (calculation for $E_{pump}/E_{thr} = 4$)

Preceding the SMBS mirror (pumping)	After the SMBS mirror (Stokes line)
4	$2 \cdot 10^6$
16	$2 \cdot 10^8$
64	$5 \cdot 10^9$

Experiments [Ref. 21] (Fig. 7a, b) and calculations (Fig. 7c) have shown that the SMBS mirror eliminates the forerunner and considerably improves the energy contrast. The experimental data show that the attained contrast is greater than 10^6 (the threshold of resolution of our methods at present), while the results of calculations summarized in Table 2 imply that the radiation contrast can be increased to 10^8-10^9.

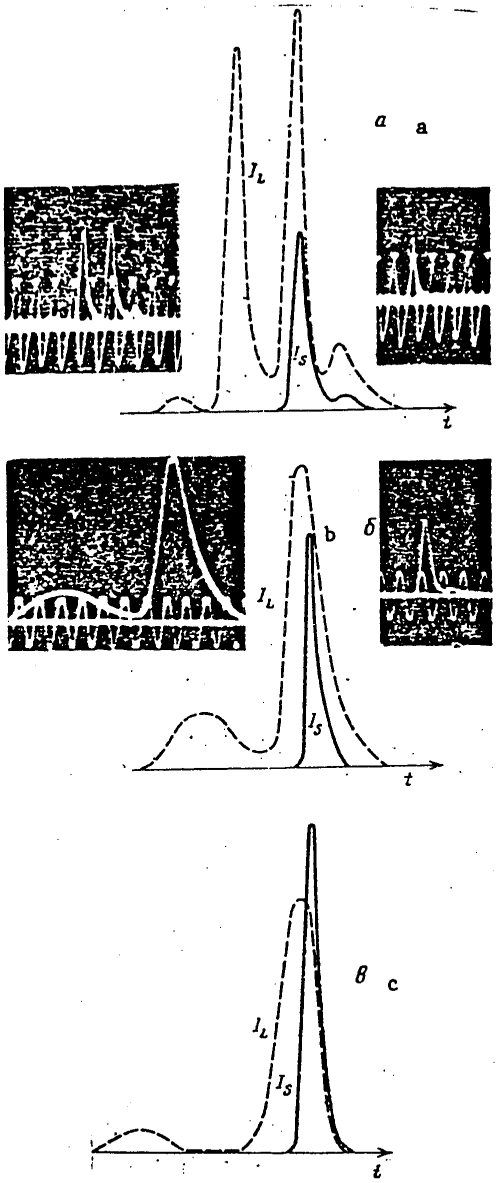

Fig. 7. Forerunner elimination and radiation pulse sharpening for iodine laser with SMBS. Broken curves -- pumping, solid curves -- Stokes radiation; a, b -- experiment; c -- calculation

4. Methods of shortening laser pulse duration

Theoretical estimates and cumulative experience (see for example Ref. 45) show that at energies of $\leqslant 10^3$ J incident on the target the pulse duration should not exceed 0.1-0.3 ns. In this connection, let us call attention to the fact that when laser emission interacts with the SMBS mirror (see Fig. 7) there is considerable sharpening of the leading edge of the laser pulse and shortening of its duration. For example in the experiment of Fig. 7b the rise time was shortened from ~1 to ~0.2 ns (with consideration of the resolution of the instrumentation), and pulse duration was shortened from ~5 to ~1 ns.

Calculations done for conditions close to the experimental conditions have also shown that in the process of stimulated Mandelstam-Brillouin scattering the pulse duration is shortened ($\tau_S < \tau_L$) and the leading edge τ_{1e} is sharpened (see Fig. 7c). The steepness of the leading edge depends appreciably on the excess of pumping energy over the threshold value ($\tau_{1e} = 1$ ns at $E_p/E_{th} = 1.4$, and $\tau_{1e} = 0.2$ ns at $E_p/E_{th} = 14$).

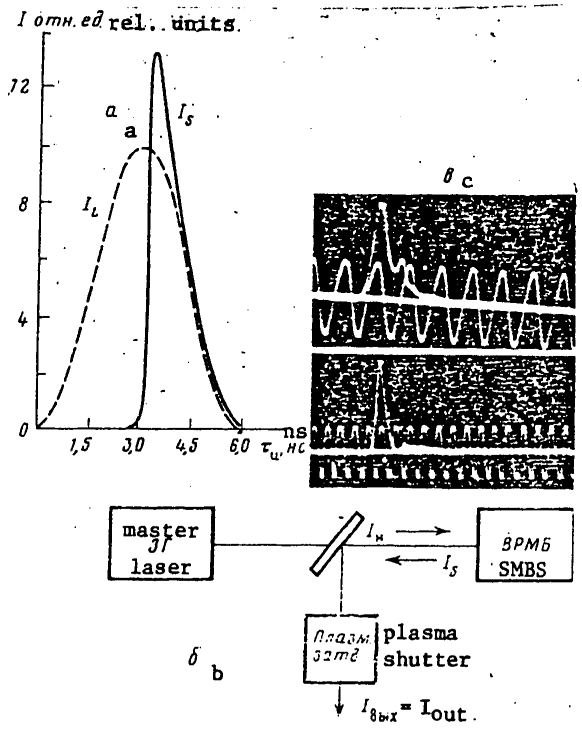

Fig. 8. Shortening the duration of iodine laser pulse radiation by stimulated Mandelstam-Brillouin scattering and a plasma shutter; a--calculation; b--experimental setup; c--experimental results

The profiles of pumping and Stokes-line emission shown in Fig. 8 correspond to $E_p/E_{th} = 4$. It can be seen that the leading edge is shortened by nearly an order of magnitude, while the remainder of the profile practically repeats the shape of the stimulating radiation pulse.

On the basis of the results, a master laser was developed for producing pulses with controllable duration by using a plasma shutter to cut off the trailing edge [Ref. 46] in the setup described above with SMBS mirror. As a result, the shaped radiation pulse had a duration (with consideration of the resolution of the equipment) of ~350-500 ps with energy up to 0.1 J (see Fig. 8). Shortening of laser pulse duration with a steep leading edge may also be done during propagation in the amplification stages operating under conditions of sufficiently strong saturation.

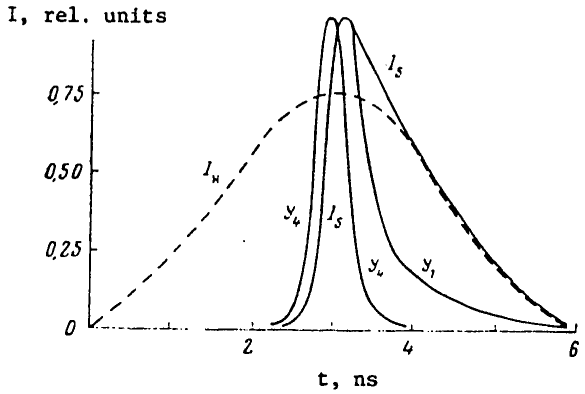

Fig. 9. Shortening of duration of Stokes pulse during amplification ($\tau_p = 3$ ns, $\tau_S = 1.1$ ns, $\tau_{y_1} = 0.5$ ns, $\tau_{y_4} = 0.3$ ns)

Calculations of the type of Ref. 23 showed (see Fig. 9) that a laser pulse having half-amplitude duration $\tau_L = 3$ ns and shortened by stimulated Mandelstam-Brillouin scattering to $\tau_S = 1.1$ ns is further shortened to 0.3 ns in the amplification process. To shorten the duration of the iodine laser pulse to $\tau \approx 10^{-10}$ s one can use the method of attenuation of free polarization (free induction) proposed in Ref. 47 and realized for the iodine laser in Ref. 46.

In our experiments, which were analogous to those of Ref. 46, radiation with duration of ~2.5 ns and energy of 0.4 J was sent from a master laser (ML) with preamplifier (Fig. 10a) to a plasma shutter. From there a pulse with steep trailing edge formed as a result of optical breakdown (Fig. 10b) was sent to an iodine shutter [Ref. 8, 20] that cut off the flat leading edge (Fig. 10c). The result was a pulse with duration at half-amplitude of about $3 \cdot 10^{-10}$ s. Analysis of the results with consideration of the time resolution of the equipment enabled evaluation of the upper limit of duration of the pulse leaving the iodine shutter, which was 120 ps*. Output energy was 1-3 mJ at an input energy of 10-15 mJ.

*In this connection it should be borne in mind that the minimum pulse duration limited by bandwidth in an iodine laser is ~40-100 μs·atm [Ref. 17, 48].

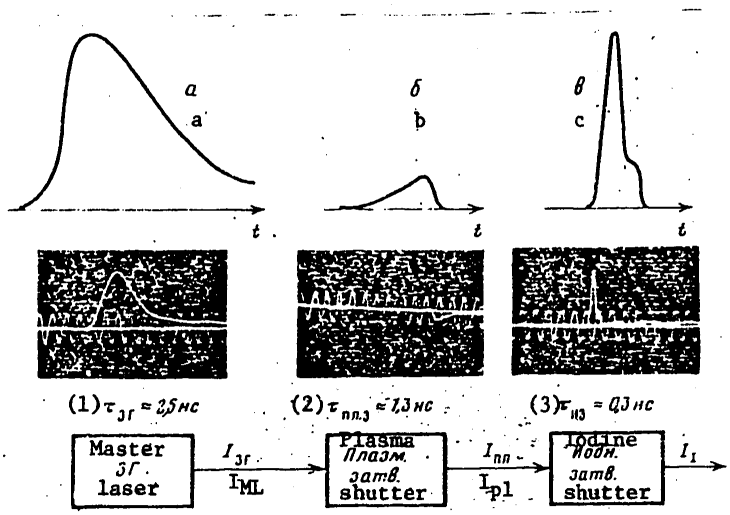

Fig. 10. Use of plasma and iodine shutters to shorten the duration of the emission pulse of an iodine laser

KEY: 1--$\tau_{ML} \approx 2.5$ ns
2--$\tau_{pl.sh.} \approx 1.3$ ns
3--$\tau_{iod.\ sh.} \approx 0.3$ ns

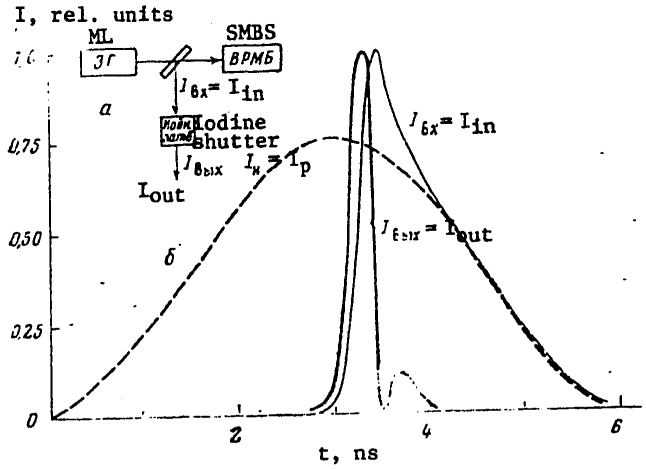

Fig. 11. Shortening the duration of the Stokes-line pulse in an iodine laser: a--equipment; b--calculation: $\tau_p = 3$ ns; $\tau_{in} = 1$ ns; $\tau_{out} = 0.25$ ns

Combining the SMBS mirror with the iodine shutter (Fig. 11a) gives an interesting possibility for shaping a laser pulse of short duration. To do this, the pulse reflected by the SMBS mirror with steep leading edge must be sent to a passive shutter with narrow absorption line that passes the leading edge of the pulse and filters out its flat trailing edge. This possibility has been checked and verified by calculation (Fig. 11b). It should be noted that the contrast may be very high in the proposed method.

5. The Iskra-IV high-power iodine laser.

The high-power iodine laser that we are developing consists of a master laser and four amplifiers of increasing diameter and length. The master laser, which produces a pulse with the required duration and contrast, consists of the laser proper with active Q-switching, two preamplifiers pumped by hollow lamps, and four Kerr cells: a modulating cell, a cutoff cell and two decoupling cells.

The relatively weak input signal arriving from the master laser is preamplified in the first two amplifiers Y_1 and Y_2 in which the working medium to be pumped by the lamps is contained in quartz cells. Amplifiers Y_3 and Y_4 are intended for getting the maximum output energy in the monopulse mode, and in this connection they have relatively large overall dimensions. This makes it possible to get high output energy in a single beam, which in turn optimizes both the number of stages and the number of beams for irradiating a target at a given energy.

Repeat-action electrodischarge sources [Ref. 15] are used for circulating the large cross sections of active medium in these amplifiers. Amplifiers Y_3 and Y_4 consist of two or more sections. Around each section, on a circle with diameter of about 40 cm, are 9 sources each 2 m long. An electric energy of 65 and 85 kJ (in Y_3 and Y_4 respectively) is sent to each source from a specially developed capacitive accumulator with stored energy of about 4 MJ. Its characteristics make this accumulator one of a kind: with voltage of 50 kV and energy capacity of about 4 MJ the duration of the discharge half-period is less than 40 μs. And experiments have shown that about 70% of the electric energy stored in the accumulator is released in the first half-peiod. The perfluoroalkyl iodide $p\text{-}C_3F_7I$ mixed with various buffer gases (CO_2, SF_6, Ar) was taken as the working substance for all stages. The pressure of the components of the working mixture was chosen in such a way that the weak-signal gain did not exceed 100. To prevent self-excitation and improve the spatial structure of the beam, decoupling mechanisms P_1 and P_2 were connected at the output of amplifiers Y_1 and Y_2. These decouplers were passive shutters combined with spatial selectors. Phototropic bismuth coatings are now used as the passive shutters.

Without going into detail as to the results of the experimental study of the master laser and each of the amplifiers individually, we give the results of experiments in which the operation of the laser as a whole was studied in the monopulse mode (Table 3).

We can see from the table that results close to those anticipated were realized even in the first experiments. The radiation energy obtained at the output of the final stage is greater than that produced in a single beam on any other type of laser at $\tau \approx 10^{-9}$ s. The efficiency of utilization of the accumulator energy is 0.1%. Beam divergence on the 80% energy level was $3 \cdot 10^{-4}$ radian. Radiation energy contrast exceeded 10^6.

TABLE 3

Stage	Version 1				Version 2			
	$\phi_{il} \times la$, cm	$P_{C_3F_7I}$	K_0	E_{out}, J*	$\phi_{il} \times la$, cm	$P_{C_3F_7I}$	K_0	E_{out}, J*
ML	1.6×80	50	1000	0.5	1.6×80	50	1000	0.5
Y_1	3.6×100	30	300	6 (7)	3.6×100	30	360	5 (7)
Y_2	8×200	22	77	33 (30)	8×200	22	140	30 (30)
Y_3	40×400	4.5	90	360 (390)	40×400	4.5	100	300 (320)
Y_4	-	-	-	-	50×400	4.5	125	1400 (1600)

The results given here show that many capabilities of iodine lasers have been successfully realized. However, there are still many problems waiting to be solved: Increasing contrast to 10^7-10^8, shortening pulse duration to 0.1-0.3 ns, raising laser efficiency to 0.3-0.5%, reducing beam divergence to ~10^{-4} radian, improving the spatial structure of the beam, developing optically stable reflective and phototropic coatings for the optical elements of amplifiers and the reprojecting optics.

Cumulative experience and the results of research done both in the Soviet Union and elsewhere indicate that these problems can be solved, which makes the iodine laser a useful tool for studying the crucial problems of laser-driven fusion.

REFERENCES

1. S. G. Rautian, V. I. Sobel'man, ZHURNAL EKSPERIMENTAL'NOY I TEORETICHESKOY FIZIKI, Vol 41, 1961, p 2018.

2. J. V. Kasper, G. C. Pimental, APPL. PHYS. LETTS, Vol 5, 1964, p 231.

3. T. L. Andreyeva, V. A. Dudkin, V. I. Mal'yshev et al., ZHURNAL EKSPERIMENTAL'NOY I TEORETICHESKOY FIZIKI, Vol 49, 1965, p 1408.

4. A. J. De Maria, C. J. Ultee, APPL. PHYS. LETTS, Vol 9, 1965, p 67.

5. C. M. Perar, APPL. PHYS. LETTS, Vol 12, 1968, p 381.

6. P. Gensel, K. Hohla, K. L. Kompa, APPL. PHYS. LETTS, Vol 18, 1971, p 48.

7. N. G. Basov, L. Ye. Golubev, V. S. Zuyev et al., KVANTOVAYA ELEKTRONIKA, No 6 (18), 1973, p 116.

8. V. A. Gaydysh, G. A. Kirillov, S. B. Kormer et al., PIS'MA V ZHURNAL EKSPERIMENTAL'NOY I TEORETICHESKOY FIZIKI, Vol 20, 1974, p 243.

9. F. I. Alridge, APPL. PHYS. LETTS, Vol 22, 1973, p 180.

10. R. E. Palmer, H. A. Gusinow, IEEE J. QUANT. ELECTRON., QE-10, 1974, p 615.

11. H. J. Baker, T. A. King, J. PHYS. D, Vol 8, 1975, p 131.

12. G. Brederlow, K. I. Witte, E. Fill et al., IEEE J. QUANT. ELECTRON., QE-12, 1976, p 152.

13. LASER FOCUS, Vol 2, 1976, p 4.

14. N. G. Basov, V. S. Zuev, V. A. Katulin et al., "Laser und ihre Anwendungen," Dresden, 1977, p 52.

15. A. V. Belotserkovets, V. A. Gaydash, G. A. Kirillov et al., PIS'MA V ZHURNAL TEKHNICHESKOY FIZIKI, Vol 5, 1979, p 204.

16. K. Hohla, G. Brederlow, E. Fill et al., Max-Planck Institut für Plasma Physik, IPP IV/93, 1976.

17. W. Fuss, K. Z. Hohla, NATURFORSCH., Vol 31a, 1976, p 569; W. Fuss, K. Hohla, Institut für Plasma Physik, Report IPP IV/67, Garching, Germany, 1974.

18. K. Hohla, "Laser-75 Opt-Electron. Conf. Proc.," Munich, 1975, Guildford, 1976, p 52.

19. J. Willson, D. O. Ham, LASER FOCUS, Vol 12, No 11, 1976, p 38.

20. V. A. Gaydash, V. A. Yeroshenko, S. G. Lapin et al., KVANTOVAYA ELEKTRONIKA, Vol 3, 1976, p 1701.

21. S. B. Kormer, S. M. Kulikov, V. D. Nikolayev et al., PIS'MA V ZHURNAL TEKHNICHESKOY FIZIKI, Vol 5, 1979, p 213.

22. L. I. Zykov, G. A. Kirillov, S. B. Kormer et al., KVANTOVAYA ELEKTRONIKA, Vol 4, No 6, 1977, p 1336.

23. Yu. V. Dolgopolov, Yu. F. Kir'yanov, S. B. Kormer et al., in: "Obrashcheniye volnovogo fronta opticheskogo izlucheniya v nelineynykh sredakh" [Wavefront Reversal of Optical Radiation in Nonlinear Media], Institute of Applied Physics of the USSR Academy of Sciences, 1979.

24. L. I. Zykov, G. A. Kirillov, S. B. Kormer et al., ZHURNAL EKSPERIMENTAL'NOY I TEORETICHESKOY FIZIKI, Vol 67, No 3(9), 1974, p 902.

25. A. I. Zaretskiy, G. A. Kirillov, S. B. Kormer, S. A. Sukharev, KVANTOVAYA ELEKTRONIKA, Vol 1, 1974, p 1185.

26. G. A. Kirillov, S. B. Kormer, G. G. Kochemasov et al., KVANTOVAYA ELEKTRONIKA, Vol 2, 1975, p 666.

27. L. I. Zykov, G. A. Kirillov, S. B. Kormer et al., KVANTOVAYA ELEKTRONIKA, Vol 2, 1975, p 123.

28. Yu. V. Dolgopolov, V. A. Komarevskiy, S. B. Kormer et al., ZHURNAL EKSPERIMENTAL'NOY I TEORETICHESKOY FIZIKI, Vol 76, 1979, p 908.

29. S. B. Kormer, V. D. Nikolayev, N. N. Rukavishnikov, S. A. Sukharev, PIS'MA V ZHURNAL TEKHNICHESKOY FIZIKI, Vol 5, 1979, p 1416.

30. J. Vevges, SPECTROCHIMICA ACTA, Vol 24B, No 3, 1979, p 177; I. M. Belousova, V. M. Kiselev, V. N. Kurzenkov, OPTIKA I SPEKTROSKOPIYA, Vol 33, 1972, p 203; V. S. Zuyev, V. A. Katulin, V. Yu. Nosach, O. Yu. Nosach, ZHURNAL EKSPERIMENTAL'NOY I TEORETICHESKOY FIZIKI, Vol 62, 1972, p 1673.

31. V. A. Alekseyev, T. L. Andreyeva, V. N. Volkov, Ye. A. Yukov, ZHURNAL EKSPERIMENTAL'NOY I TEORETICHESKOY FIZIKI, Vol 63, 1972, p 453; Ye. A. Yukov, KVANTOVAYA ELEKTRONIKA, Vol 3, 1973, p 117.

32. L. M. Frantz, J. S. Nodvik, J. APPL. PHYS., Vol 34, 1973, p 2346; P. V. Avizonis, R. L. Grotbeck, J. APPL. PHYS., Vol 37, 1966, p 687.

33. S. M. Andreyev, S. G. Baykov, P. N. Dashuk et al., OPTIKO-MEKHANICHESKAYA PROMYSHLENNOST', No 5, 1972, p 19.

34. A. S. Antonov, I. M. Belousova, V. A. Gerasimov et al., PIS'MA V ZHURNAL TEKHNICHESKOY FIZIKI, Vol 4, 1978, p 1143.

35. B. V. Alekhin, B. V. Lazhintsev, V. A. Nor-Averyan et al., KVANTOVAYA ELEKTRONIKA, Vol 3, 1976, p 2369.

36. A. V. Zaretskiy, L. I. Zykov, G. A. Kirillov et al., KVANTOVAYA ELEKTRONIKA, Vol 6, 1979, p 1278.

37. N. G. Basov, V. S. Zuyev, V. A. Katulin et al., KVANTOVAYA ELEKTRONIKA, Vol 6, No 2, 1979, p 311.

38. I. M. Belousova, O. B. Danilov, I. A. Sinitsyn, V. V. Spiridonov, ZHURNAL EKSPERIMENTAL'NOY I TEORETICHESKOY FIZIKI, Vol 58, 1970, p 1481.

39. E. Fill, K. Hohla, OPT. COMMUNS., Vol 18, 1976, p 431.

40. M. P. Vanyukov, V. I. Isayenko, P. P. Pashinin et al., KVANTOVAYA ELEKTRONIKA, No 1, 1971, p 35.

41. B. Ya. Zel'dovich, V. I. Popovichev, V. V. Ragul'skiy, F. S. Fayzullov, PIS'MA V ZHURNAL EKSPERIMENTAL'NOY I TEORETICHESKOY FIZIKI, Vol 15, 1972, p 160.

42. O. Yu. Nosach, V. I. Popovichev, V. V. Ragul'skiy, F. S. Fayzullov, PIS'MA V ZHURNAL EKSPERIMENTAL'NOY I TEORETICEHSKOY FIZIKI, Vol 16, 1972, p 617.

43. Yu. I. Kruzhilin, KVANTOVAYA ELEKTRONIKA, Vol 5, 1978, p 625.

44. V. S. Zuyev, V. A. Katulin, V. Yu. Nosach, O. Yu. Nosach, ZHURNAL EKESPERIMENTAL'NOY I TEORETICHESKOY FIZIKI, Vol 62, 1972, p 1673.

45. J. A. Maniscalco, Lawrence Livermore Laboratory, Report UCRL-76763, Livermore, California, 1975; Lawrence Livermore Laboratory, Laser Program Annual Report, 1976, UCRL-50021-76, Livermore, Calif., 1977; Lawrence Livermore Laboratory, Laser Program Annual Report, 1977, v. 1, 2, UCRL-50021-77, Livermore, Calif., July, 1978.

46. E. Fill, K. Hohla, G. T. Schappert, R. Volk, APPL. PHYS. LETTS, Vol 29, 1976, p 805.

47. E. Yablonovitch, I. Goldhaar, APPL. PHYS. LETTS, Vol 25, 1974, p 580.

48. E. P. Jones, M. A. Palmer, F. R. Franklin, OPT. QUANT. ELECTRON., No 8, 1976, p 231.

6610
CSO: 8144/0285

UDC 678.7.352

CHEMICAL LASERS: NEW RESULTS AND IDEAS

Moscow IZVESTIYA AKADEMII NAUK SSSR: SERIYA FIZICHESKAYA in Russian Vol 44, No 8, Aug 80 pp 1554-1565

[Article by A. N. Orayevskiy, Physics Institute imeni P. N. Lebedev, USSR Academy of Sciences]

[Text] This article is based on results and ideas arrived at and elaborated in the Lebedev Physics Institute. Results found in other laboratories will be mentioned only inasmuch as they are pertinent to our research. Many details of design and principles of operation of chemical lasers are omitted. This type of information is now readily accessible in a number of books that have already been published [Ref. 1-3]*.

Chemical cw lasers

Fig. 1 shows a schematic diagram of a cw chemical laser that has now become conventional for lasers based on reaction of atomic fluorine with hydrogen:

$$F + H_2 \rightarrow HF^* + H. \quad (1)$$

Major parameters that have been realized up to this point in a number of laboratories are summarized in Table 1.

Fig. 2 shows a diagram of a purely chemical DF-CO_2 laser utilizing initiation of a chain reaction in a mixture of $D_2 + F_2$ by the NO radical. Such a laser has been studied by many authors at subsonic discharge of reagents. Laser parameters are summarized in Table 2.

Supersonic versions of the DF-CO_2 laser are also known, both with gas generator initiation [Ref. 2, 3] and with initiation by the NO radical [Ref. 4] (Table 3). The latter is of interest because of its high pressure (233 mm Hg), although it has lower chemical efficiency (~1.9%) than the subsonic version (4-5%).

Many questions arise in connection with the utilization of lasers of this type. Among these questions are the following. Can the specific energy output be increased, or have limiting parameters already been attained? Can the pressure in

*Ref. 2 was translated into Russian this year [Mir publishers, Moscow, 1980).

the cavity be increased without impairing the laser characteristics? Can another system be found that is energetically comparable with the HF laser but with non-toxic reaction products? This part of our article will be devoted to development of a number of ideas that give an affirmative answer to these questions.

TABLE 1

HF laser

1. Specific energy ε	150-200 $J \cdot g^{-1}$
2. Static pressure p in the laser cavity	5 mm Hg
3. Flow velocity v	$2 \cdot 10^5$ $cm \cdot s^{-1}$
4. Typical molecular composition of the mixture $[F]:[H_2]:[He]$ in the laser cavity	1:9:10

TABLE 2

DF-CO_2 laser

1. Specific energy ε	50-60 $J \cdot g^{-1}$
2. Static pressure p in the laser cavity	15 mm Hg
3. Flow velocity v	$2 \cdot 10^4$ $cm \cdot s^{-1}$
4. Initiating process	$NO + F_2 \rightarrow F + NOF$
5. Molar composition of the mixture $[F_2]:[D_2]:[CO_2]:[He]$ in the laser cavity	1:1:8:15

TABLE 3

Total power P	1.45 kW
Flow of reagents	
F_2	5.29 g s^{-1}
CO_2	57.8 g s^{-1}
D_2	1.61 g s^{-1}
He	15.1 g s^{-1}
NO	1.53 g s^{-1}
Pressure p in laser cavity	233 mm Hg
Temperature in initiation chamber	300 K
Chemical efficiency	1.9%
Mach number M at nozzle tip	1.5

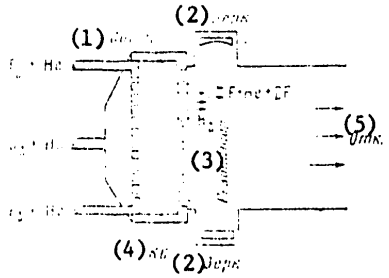

Fig. 1

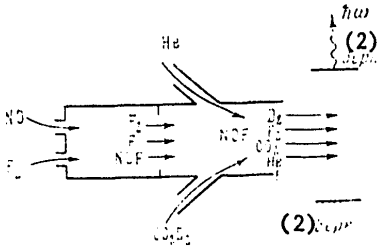

Fig. 2

Fig. 1. Schematic diagram of a cw chemical HF laser

Fig. 2. Schematic diagram of a cw chemical DF-CO_2 laser

KEY: 1--Nozzle
2--Mirror
3--Laser cavity
4--Combustion chamber
5--Evacuation

The main reserve for increasing the specific energy (power) of a cw laser is in the use of a chain reaction of hydrogen with fluorine. The reaction between hydrogen and fluorine develops in a chain mechanism

$$F + H_2 \rightarrow HF^* + H \text{ (32 kcal mol}^{-1}\text{ HF)},$$
$$H + F_2 \rightarrow HF^* + F \text{ (98 kcal mol}^{-1}\text{ HF)}. \qquad (2)$$

We noted previously that the development of chemical lasers has taken the path of utilization of the former of these reactions. But if the second stage of this reaction is used, by adding a sufficient amount of molecular fluorine to the mixture, the average energy per HF molecule increases to 65 kcal mol^{-1}. It turns out that converting to the chain-reaction mode promises to more than double the specific power characteristics of the laser. If consideration is also taken of the fact that the initial amount of atomic fluorine has to be less for the chain-reaction process, then the specific power output should be even more appreciable [Ref. 5, 6]. A "savings" is possible on this basis. The fewer the atoms of fluorine, the less the "fuel" expended on creating them, the less the reaction products that deactivate the active molecules in the laser cavity. The fewer the atoms of fluorine, the more slowly the reaction develops, and the better the mixing process can be organized.

Shown in Fig. 3 are the results of calculation of che behavior of gain in the chain-reaction HF laser along the flow of the jet [Ref. 6]. It can be seen that at low initial fluorine concentrations the reaction is noticeably delayed, which increases the time reserve for more effective intermixing of the jets. Such arguments in favor of chain-reaction lasers prompt the question: why haven't they already come into use, the moreso as chemical lasers have been successfully using the advantages of the chain-reaction process for a long time now? The answer to

this question is that development of a cw chemical laser based on a chain reaction requires overcoming a number of difficulties, the most fundamental being the heat crisis of supersonic flow. In this phenomenon, as heat is released in a supersonic jet of constant cross section it loses velocity, and the supersonic flow may be interrupted, accompanied by an abrupt rise in temperature in the jet, which in the final analysis leads to interruption of lasing.

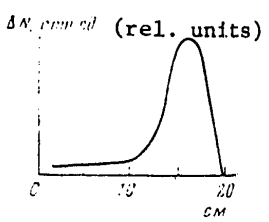

Fig. 3

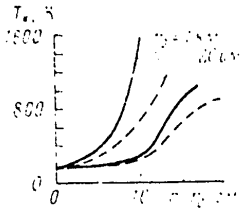

Fig. 4.

Fig. 3. Downstream development of inverse population ΔN for chain-reaction HF laser. The distance from the nozzle tip is laid off along the axis of abscissas.

Fig. 4. Temperature of the jet of reacting flow in HF laser with cylindrical nozzle array as a function of distance from the nozzle array (chain reaction)

A helium diluent is used in the cw chemical laser to eliminate the flow heat crisis. But when the chain reaction is used, the heat release in the laser zone rises sharply, and the problem of the flow heat crisis becomes much more complicated. Dilution of the flow would lead to an increase in helium expenditure and a reduction of specific power output. Another method, separation of jets, severly increases the dimensions of the system.

The most effective way out of this difficulty is to use a cylindrical configuration in the nozzle array. At the Lebedev Physics Institute, detailed calculations have been done on a cw HF laser with initiation by a nozzle array [Ref. 7]. Equations of gasdynamics and of the usual kinetics of a chemical laser were simultaneously solved in this research. In doing this, consideration was taken of flux, diffusion, viscosity and thermal conductivity of the jets. The equations used in Ref. 7 were written in the boundary layer approximation. The justification for this approach is the small transverse dimension of the intermixing jets. The most interesting results of the work are discussed below.

Shown in Fig. 4 is the behavior of the jet temperature along the flow as a function of the radius r_0 of the cylindrical nozzle array. An abrupt rise in flow temperature in the case of a flat nozzle array ($r_0 = 10^5$ cm) begins almost immediately beyond the tip of the nozzle units, whereas for a radius $r_0 = 20$ cm the temperature is retained up to distances $r - r_0 = 10$-12 cm which are of practical interest. The temperature rise in the vicinity of 12-15 cm at $r_0 = 20$ cm is not as abrupt and catastrophic as for a flat nozzle assembly. Let us note that the emission, in coupling out part of the energy of the flow, helps to eliminate the flow crisis. Calculations show that at $\beta_{He} = [He]/[F_2] = 10$ and $r_0 \geqslant 10$ cm in the absence of lasing

a flow crisis sets in, whereas there is no such crisis in the lasing mode even when $r_0 = 20$ cm, as can be seen from Fig. 4. Emission has a considerable effect on gas dynamics.

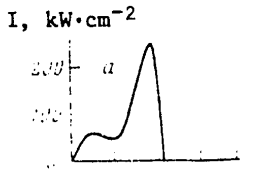

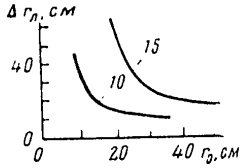

Fig. 6

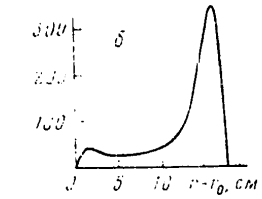

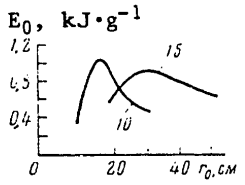

Fig. 5 Fig. 7

Fig. 5. Intensity distribution along the flow for radiation of an HF laser with cylindrical nozzle assembly (chain reaction): a--radius r_0 of nozzle unit 30 cm; b--radius of nozzle unit 15 cm. Pressure in the cavity 15 mm Hg; $\beta_{He}=[He]/[F_2]_0=10$; $[F_2]_0$ is the initial concentration of fluorine molecules in the combustion chamber (gas generator)

Fig. 6. Width of radiation band of the HF laser as a function of the radius of a cylindrical nozzle unit (chain reaction). The numbers near the curves show the values of β_{He}

Fig. 7. Specific radiation energy of HF laser as a function of the radius of the cylindrical nozzle unit (chain reaction). Notation same as in Fig. 6 .

Fig. 5 shows the distribution of intensity of HF laser emission integrated over the entire radiation spectrum. The intensity distribution along the flow that is characteristic of a chain reaction is retained in the cylindrical version as well. As the radius increases, the distribution is compressed along the flow. This circumstance is reflected by Fig. 6, which shows how the width of the lasing band $\Delta r_л$ depends on r_0.

Finally, Fig. 7 shows important results of calculation of the specific energy behavior of a laser with a cylindrical cavity. It can be seen that for each degree of dilution β_{He} there is an optimum radius of the nozzle unit for which the specific power output is maximum. Calculation shows that the maximum specific power output may reach considerable values of 800-1000 J·g^{-1} at a pressure of p = 15 mm Hg on the tip of the nozzle assembly. Thus using the chain reaction of hydrogen with fluorine in combination with a cylindrical configuration of the nozzle array can appreciably improve the characteristics of cw chemical lasers.

The search for chemical lasing mixtures with nontoxic discharge has been to some extent successful, with a good outlook for progress in solving this problem. The following exposition will show what we mean by this statement.

Joint research by the Lebedev Physics Institute and Moscow Engineering Physics Institute on the OD-CO_2 laser, which was first discovered in Ref. 8 showed that this laser has good potential capabilities [Ref. 9-12]. The laser is pumped by the process

$$\begin{aligned} D + O_3 &\rightarrow OD^* + O_2, \\ OD^* + CO_2 &\rightarrow OD + CO_2^*. \end{aligned} \qquad (3)$$

The lasing molecule is CO_2. The end products of the reaction (O_2, CO_2, D_2O) are nontoxic. The characteristics of such a laser were studied on the facility diagrammed in Fig. 8 [Ref. 12]. Atomic hydrogen was produced in shock tube 1 behind the wave front of the shock wave propagating in the mixture of $Ar + D_2$ after reflection from diaphragm 2. The hot mixture of $Ar + D_2 + D$ was discharged from the nozzles of the cellular nozzle array and mixed with a stream containing $CO_2 + O_3 + He$. Different mixing arrangements were studied. Among the investigated designs, the best results were obtained with the mixer diagrammed in Fig. 9 with parameters shown in Table 4.

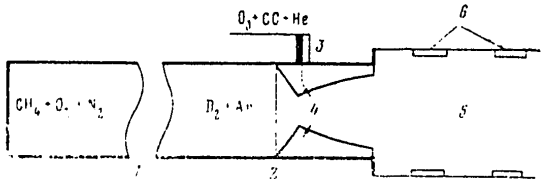

Fig. 8. Diagram of experimental OH(OD)-CO_2 laser: 1--shock tube; 2-- diaphragm; 3--electric valve for injection of mixture of $O_3 + CO_2 + He$; 4--nozzle array; 5--active lazer zone; 6--windows for coupling out laser emission

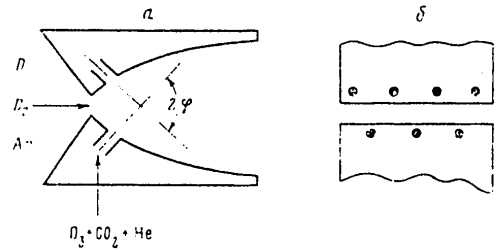

Fig. 9. Design of the nozzle array of the OH(OD)-CO_2 laser: a--side view across the flow; b--end view of the nozzle (orifices for injection of $O_3 + CO_2 + He$ mixture are displaced relative to one another in the upper and lower parts of the nozzle)

Thus Table 4 shows that the supersonic OD-CO_2 laser has a considerable specific power output, a fairly extended lasing zone and high static pressure in the cavity. At first glance, it seems to have a specific energy output about half the level of the DF-CO_2 laser. However, in reality the specific energy of the OD-CO_2 laser can be appreciably improved if Ar is eliminated from the mixture, as it is not essential and is only there because of the method used for getting atomic deuterium. When we recalculate for helium, we get a specific energy of 60 $J \cdot g^{-1}$, which is on the level of this parameter for the DF-CO_2 laser.

TABLE 4

Composition for the mixture of $[O_3+O_2]:[CO_2]:[He]$	1:12:30
Gain κ	2.65 ± 0.13 m^{-1}
Specific energy ε	35 J·g^{-1}
Pressure p in laser cavity	15 mm Hg
Flow velocity v	$1.8 \cdot 10^5$ cm·s^{-1}
Width of inversion zone along the flow	20 cm
Lasing time τ	2 ms
Total lasing power P	960 W
Nozzle dimensions	
h_{cr}	0.45 mm
h_{out}	2.7 cm

One of the most interesting results of the studies done in Ref. 12 is the discovery that substituting hydrogen for deuterium does not cause any appreciable fall-off in laser characteristics. An experiment showed [Ref. 12] that the OH-CO_2 laser has a gain only 8% lower than that of the OD-CO_2 laser, and nearly the same specific energy output. This is an important factor that increases interest in the OH-CO_2 laser.

In order to give the proposed laser the appearance of a structurally finished system it is necessary to learn how to produce atomic hydrogen by a chemical method. Our calculations showed that the required concentrations of hydrogen can be obtained by utilizing combustion of hydrogen in oxygen. All these factors show the promise of research on developing a purely chemical OH-CO_2 laser with nontoxic discharge products.

In discussing the recent advances in the field of cw chemical lasers, we must not overlook the development of a purely chemical laser by U. S. researchers [Ref. 13, 14]. The radiative transition in this laser is

$$I(P_{3/2}) \rightarrow I(P_{1/2}) + h\nu, \tag{4}$$

Atomic iodine in state $P_{1/2}$ is obtained by transmission of a quantum of energy from singlet oxygen

$$O_2(^1\Delta) + I(P_{3/2}) \rightarrow O_2(^3\Sigma) + I(P_{1/2}). \tag{5}$$

Since $P_{3/2}$ is the ground state, inversion results from the excess of quantum $O_2(^1\Delta)$ over the quantum necessary for excitation of $I(P_{1/2})$.

And finally, the most striking part of this arrangement is that atomic iodine is obtained from molecular I_2 due to the energy of singlet oxygen

$$2O_2(^1\Delta) + I_2 \rightarrow 2O_2(^3\Sigma) + 2I(P_{1/2}). \tag{6}$$

Oxygen in state $^1\Delta$ is produced by the well known reaction of chlorinating hydrogen peroxide [Ref. 15]. It is difficult as yet to predict the future of this laser. One thing is certain: its development involves a number of ideas that widen our concepts in the field of kinetics.

Pulsed chemical lasers

One of the major advances in the field of pulsed chemical lasers over the last two or three years is a deeper understanding of the processes that take place in the reactor and that influence the characteristics of the chemical laser. It was shown in particular that rapid establishment of rotational equilibrium of the lasing molecule is conducive to an increase in the power output and efficiency of the lasers [Ref. 16, 17]. The use of vibrational-rotational transitions with a large rotational quantum number ($J \approx 10$-15) for lasing and amplification should increase the power output and efficiency under conditions of rotational equilibrium [Ref. 18].

At the same time, it has been shown that rotational equilibrium is not established in HF molecules during the time of the lasing pulse in a laser medium of widely used composition [Ref. 19-26], so that the problem arises of adding an effective "relaxer" of rotational levels to the mixture. It was shown in Ref. 17 that the addition of such a relaxer is actually conducive to improvement of the efficiency and energy output of the chemical laser. In some papers, theoretical models that account for the finite time of establishment of rotational equilibrium have been developed on the basis of measured cross sections of rotational relaxation [Ref. 17, 27, 28].

A more precise understanding on the part of experimenters concerning the particulars of different methods of initiating chemical lasers has led to appreciable improvement of technical efficiency and power output. Table 5 summarizes results found at the Lebedev Physics Institute in studying pulsed chemical lasers with various methods of initiation.

TABLE 5

Mixture	Method of initiation	η_{chem}, %	η_{el}, %	τ, s	p, atm	ε, J/l	E, J	Ref.
$D_2+F_2+CO_2+He$	UV radiation of an open creeping discharge	7	15	$5\cdot10^{-6}$	1	150	20	29
	Electron beam	3.5	330	$4\cdot10^{-6}$	1	60	7	30
H_2+F_2+He	UV radiation of flashlamps	3.5	25	$4\cdot10^{-6}$	1	25	125	31
	Electron beam	5	960	10^{-6}	1	100	13	32

Most of these results are record-breaking. Among non-Soviet studies, we can mention the following. Ref. 33 reported attainment of an efficiency of 370% in an electronically initiated laser, but at a specific energy output of 50 J/l. The authors of Ref. 34 were able to noticeably improve the specific energy output by

a sharp increase in the degree of initiation. Although the authors of Ref. 34 do not cite this parameter, the experimental data indicate a specific energy output of the order of 300-500 J/ℓ. This result was attained at the cost of a reduction in efficiency to 180%. Let us note in passing that the overall lasing energy of 4.5 kJ attained in Ref. 34 is so far the greatest value of this parameter published for HF lasers.

Ref. 35 by U. S. researchers reported on attainment of an efficiency of about 30% with respect to energy initiation in an HF laser at a specific energy output of 22 J/ℓ. From the standpoint of efficiency, this is the best figure published to date. However, the results are not quite up to ours as regards specific energy output. There is room here for further progress, and there are reserves in more improved sources of UV radiation. It may be possible to use the luminescence of excimers excited by electron impact (electron beam, the electroionization method, other types of discharges).

The results given in Table 5 show that electronic initiation is more effective for HF lasers than for DF-CO_2 lasers. The reason for this is in the comparatively large absorption of electron energy by CO_2 molecules in the case of the DF-CO_2 laser, as this absorption in the best case is of no use for further development of the process.

Despite the fact that an electron beam injects the initiating energy into the mixture of reagents more economically than UV flashlamps, the latter sources are still just as attractive to experimenters because of their simplicity and low cost as compared with a source that produces a high-current electron beam. The efficiency with respect to the initiation energy introduced into the mixture is given in Table 5 for the case of electron-beam initiation. The actually realized efficiency ("from the plug-in point") is about one-fourth of this. In the first place the efficiency of the accelerator will scarcely exceed 50%. Secondly, it is difficult to combine initiation with 100% utilization of the beam in the laser reactor. With consideration of input losses, the beam utilization factor is about 50%. The efficiency of initiation by UV radiation cited in Table 5 refers to the energy stored in the capacitor bank.

Comparison of experiments with very intense initiation [Ref. 34] and with moderate initiation (see Table 5) leads us, as it were, to the conclusion that there is an alternative: either high efficiency with respect to investment of initiation energy, or else high specific energy output. This conclusion also has its theoretical basis: the principal deactivator of excited molecules in chemical lasers is the reaction product -- molecules of HF (DF). However, the chemical laser is a multiparameter system. And it turns out that by matching parameters we can find operating conditions such that this alternative does not occur for all practical purposes. It has been theoretically established [Ref. 36] that in a high-pressure DF-CO_2 lasers the composition of the mixture and degree of initiation can be matched to achieve an increase in both the specific energy output and efficiency with respect to the energy that initiates the reaction. The results of these calculations are shown in Table 6.

The effect of increasing quantum yield of lasing with an increase in pressure of the mixture as energy output increases takes place only at a sufficiently high degree of initiation ($4 \cdot 10^{16}$ cm^{-3}). At a lower degree of initiation ($2 \cdot 10^{15}$ cm^{-3})

TABLE 6

[illegible]	$P_{атм}$	ε, J/l	τ, s	f
$5.5 \cdot 10^{-6}$	1	85	$1.2 \cdot 10^{-6}$	121
	3	274	$1 \cdot 10^{-6}$	333
	10	740	$1 \cdot 10^{-6}$	1050
$2 \cdot 10^{-5}$	1	79	$2 \cdot 10^{-5}$	1160
	5	61	$1.1 \cdot 10^{-5}$	1460
	10	38	$8 \cdot 10^{-6}$	912
	15	4	$5.6 \cdot 10^{-6}$	97

Note: $D_2:F_2:CO_2:He = 1:3.8:3:4.8$, $t_0 \sim 10^{-7}$ s, t_0 is the time of initiation of the reaction, [F] is the concentration of active centers, τ is lasing pulse duration, f is the quantum yield of emitted radiation per fluorine atom

this is not observed (Table 6). It is a matter for experiment to verify the validity of this prediction.

Radical solution of the problem of attaining high efficiency with respect to initiation energy involves using branching processes.

It is well known that from the chemical standpoint a reaction in a mixture of H_2-F_2 is a branching process [Ref. 37]. This means that during the reaction itself chemically active centers are accumulated with concentration that increases in accordance with an exponential function [Ref. 37, 38]*

$$[F] = [F]_0 e^{st}. \tag{7}$$

However, because of the low rate of branching s, the part played by this process in development of lasing is small. Recently experiments were done [Ref. 39] that showed that the rate of branching increases sharply if vibrationally excited hydrogen with energy of two or more vibrational quanta participates in the branching reaction.

This brought us once more to the analysis of the possibilities of branching for development of lasing in a chemical DF-CO_2 laser since during the reaction D ($v \geqslant 2$) may arise through energy transfer from DF molecules ($v \geqslant 2$). It was found that such possibilities exist. The reaction can be initiated in two ways: 1) introducing a small concentration of DF (HF) molecules into the mixture that are stimulated by DF (HF) laser radiation and transfer their energy to molecules of D_2 (H_2); 2) weak initiation of the reaction by UV photolysis, which leads to formation of a "starting" number of DF molecules ($v \geqslant 2$). The results of the calculation are shown in Table 7 [Ref. 40]. The calculation shows that we can achieve satisfactory specific energy outputs (~40 $J \cdot l^{-1}$ atm^{-1}) with negligible expenditures of energy on initiation. Even if the efficiency of the lamp emission into the band of fluorine dissociation is of the order of 1%, the laser radiation energy will be dozens of times greater than the total expenditures of energy on initiation of the reaction.

*The exponential law is valid only in the linear stage of the reaction.

TABLE 7

IR-initiation
(DF molecules are added to the mixture; $P_{DF} \approx 1$ mm Hg)

Initiation energy, J/l	5.5	1.1	0.3
Lasing energy, J/l	36	37	36.6
Pulse duration, s	$4 \cdot 10^{-4}$	$9 \cdot 10^{-4}$	$1.6 \cdot 10^{-3}$

UV-initiation

Number of fluorine atoms per cm^3	$3 \cdot 10^{13}$	$3 \cdot 10^{12}$
Initiation energy, J/l	10^{-2}	10^{-3}
Lasing energy, J/l	43	29
Pulse duration, s	$1.2 \cdot 10^{-4}$	$3 \cdot 10^{-4}$

One might ask why this effect has not been experimentally observed. The fact is that relaxation of vibrational energy of $DF(v \geq 2)$ and $D_2(v \geq 2)$ due to V-V exchange with CO_2 molecules is an obstacle to development of the branching process. Therefore mixtures are needed with relatively large ratio of $[F_2]/[CO_2]$ and $[D_2]/[CO_2]$, and these are not the optimum mixtures if lasing is due to a straight chain. Another reason is that the branching process is very critical to the oxygen content in the mixture: for a mixture of the given composition its content should not exceed 0.3 mm Hg. Since oxygen is added to stabilize the mixture, stimulation of emission by a branching process requires solution of the problem of preparing mixtures with a very small oxygen content.

The possibility of initiating chemical reactions by IR radiation has led to advancement and formulation of the idea [Ref. 41] of photonic branching of a chemical process: if the number of emitted photons in the process of the reaction that accompanies IR radiation is greater than the number of photons required for initiation, the reaction will be a branching process. If in addition the process of emission may be stimulated, then by using a resonator to control emission we can in this way control the course of the reaction as a whole. By making use of the branched nature of the entire process, we can get considerable energies of coherent emission with expenditure of small energies on initiation of the reaction. The difference from the usual branching process is that the photon becomes not only the reaction product, as in the conventional chemical laser, but also a direct participant, ensuring development of the process.

Theoretical estimates show that chemical mixtures with a photonic branching mechanism are possible in principle. For example a mixture of $D_2 + F_2 + CO_2 + He + CH_3F$ is capable in principle of photonic branching, ensuring IR emission with energy ten times as high as that of the radiation used for initiation [Ref. 42]. Other mixtures are also possible. Unfortunately in many cases detailed analysis is made difficult by lack of data on the cross sections of elementary processes.

As a rule, the major problem in the case of photonic branching as well is stabilization of prepared mixtures. It is possible that a technique for rapid mixing of

reagents may be of assistance in solving this problem. In any event, the solution of these problems depends to a great extent on further improvement of experimental techniques.

A few words on chemical lasers in the visible band. In this area, researchers have come up against considerable difficulties. The hopes for recombination lasers* are not justified because of the small cross section of the recombination process. Some other possibilities are analyzed in Ref. 43**. Most interesting among these seems to be a chain reaction in a mixture of $H_2 + F_2 + N_2F_4$ producing excited $NF(^1\Delta)$ radicals***. The difficulty to achieving lasing in this mixture is the low probability of the transition $NF(^1\Delta) \rightarrow NF(^3\Sigma^-)$.

At the same time, chemical reactions are reliably known that lead to inversion and in the final analysis to creation of an active medium. These are the reactions of excited atoms that are extensively used in excimer lasers [Ref. 45, 46]. But the excited atoms in these lasers are obtained by the energy of an external source. This is most often an electron beam. Sources of UV radiation are also used [Ref. 46]. Reactions of unexcited atoms are also known that lead to visible and ultraviolet chemiluminescence with an appreciable quantum yield. This means that during the reaction excited electron states arise, but either there is no inversion or the gain is exceedingly small. The thought suggests itself that excited atoms can be produced by collision or by absorption of a quantum of chemiluminescence by the atoms due to the energy of an excited molecule produced in the reaction of unexcited atoms [Ref. 47]. As the excited atom enters into a reaction, it will lead to population inversion. Unfortunately, not a single specific reaction scheme that realizes this idea has yet been suggested.

In the preface to Ref. 2 the editors state that most fundamental research, at least that pertaining to HF, CO and iodine lasers, is in the concluding stage. The material presented here leads us to take exception to this statement. In any event, this is not the case as regards lasers based on a chain reaction of hydrogen or deuterium fluorination. We can expect new and interesting advances.

The author takes this occasion to thank A. S. Bashkin, N. N. Yuryshev and colleagues in groups under their leadership, and also V. I. Igoshin and V. A. Shcheglov for cooperation.

REFERENCES

1. A. S. Bashkin, V. I. Igoshin, A. I. Nikitin, A. N. Orayevskiy, "Khimicheskiye lazery. Itogi nauki i tekhniki. Ser. Radiotekhnika" [Chemical Lasers, Results of Science and Technology. Radio Engineering Series], Vol 8, VINITI, Moscow, 1975.

2. "Handbook of Chemical Lasers" edited by R. W. F. Gross and J. F. Bott, a Wiley Interscience Publication, 1976.

---

*See Ref. 1 and the literature cited there.
**This paper has a bibliography on the problems discussed there.
***Concerning this point, see also Ref. 44.

3. A. N. Orayevskiy, "Khimicheskiye lazery. Spravochnik po lazeram" [Chemical Lasers. A Handbook on Lasers], Vol 1, Chapter 1, "Sovetskoye radio", Moscow, 1978, p 158.

4. G. Emanuel, W. G. Gaskill, R. J. Reiner et al., IEEE, QE-12, No 11, 1976, p 739.

5. A. N. Orayevskiy, V. P. Pimenov, A. A. Stepanov, V. A. Shcheglov, KVANTOVAYA ELEKTRONIKA, Vol 3, No 1, 1976, p 136.

6. V. G. Krutova, A. N. Orayevskiy, A. A. Stepanov, V. A. Shcheglov, KVANTOVAYA ELEKTRONIKA, Vol 3, No 9, 1976, p 1919.

7. A. A. Stepanov, V. A. Shcheglov, KVANTOVAYA ELEKTRONIKA, Vol 6, No 7, 1979, p 1476.

8. N. G. Basov, A. S. Bashkin, V. I. Igoshin et al., PIS'MA V ZHURNAL EKSPERIMENTAL'NOY I TEORETICHESKOY FIZIKI, Vol 16, No 10, 1972, p 551.

9. A. S. Bashkin, A. N. Orayevskiy, N. M. Gorshunov et al., KVANTOVAYA ELEKTRONIKA, Vol 2, 1975, p 2092.

10. A. S. Bashkin, N. M. Gorshunov, Yu. A. Kunin et al., KVANTOVAYA ELEKTRONIKA, Vol 3, 1976, p 1142.

11. A. S. Bashkin, N. M. Gorshunov, Yu. A. Kunin et al., KVANTOVAYA ELEKTRONIKA, Vol 5, 1978, p 2656.

12. A. S. Bashkin, N. M. Gorshunov, Yu. A. Kunin at al., Preprint FIAN, No 140, 1979.

13. W. E. McDermott, N. R. Pchelkin, D. I. Benard et al., APPL. PHYS. LETTS, Vol 32, No 8, 1978, p 469.

14. D. J. Benard, "Ninth Winter Colloquium on Quantum Electronics," 8-10 January, 1979, Snow Bird, Utah.

15. H. H. Seliger, J. CHEM. PHYS., Vol 40, 1964, p 3133.

16. V. I. Igoshin, A. N. Orayevskiy, KRATKIYE SOOBSHCHENIYA PO FIZIKE, FIAN SSSR, No 7, 1976, p 27.

17. G. K. Vasil'yev, Ye. F. Makarov, A. G. Ryabenko, V. L. Tal'roze, ZHURNAL EKSPERIMENTAL'NOY I TEORETICHESKOY FIZIKI, Vol 71, No 4(10), 1976, p 1320.

18. V. I. Igoshin, A. N. Orayevskiy, PIS'MA V ZHURNAL EKSPERIMENTAL'NOY I TEORETICHESKOY FIZIKI, Vol 21, 1975, p 235.

19. L. M. Peterson, G. H. Lindquist, C. B. Arnold, J. CHEM. PHYS., Vol 61, No 8, 1974, p 3480.

20. G. K. Vasil'yev, Ye. F. Makarov, A. G. Ryabenko, V. L. Tal'roze, ZHURNAL EKSPERIMENTAL'NOY I TEORETICHESKOY FIZIKI, Vol 68, No 4, 1975, p 1241.

21. J. J. Hinchen, APPL. PHYS. LETTS, Vol 27, No 12, 1975, p 672.

22. V. I. Gur'yev, G. K. Vasil'yev, O. M. Batovskiy, PIS'MA V ZHURNAL EKSPERIMENTAL'NOY I TEORETICHESKOY FIZIKI, Vol 23, No 5, 1976, p 256.

23. J. J. Hinchen, R. H. Hobbs, J. CHEM. PHYS., Vol 65, No 7, 1976, p 2732.

24. N. C. Lang, J. C. Polanyi, J. Wanner, CHEMICAL PHYSICS, Vol 24, 1977, p 219.

25. G. K. Vasil'yev, V. I. Gur'yev, A. O. Koval'skiy, ZHURNAL PRIKLADNOY SPEKTROSKOPII, Vol 30, No 6, 1979, p 1048.

26. J. J. Hinchen, R. H. Hobbs, J. APPL. PHYS., Vol 50, No 2, 1979, p 628.

27. R. L. Kerber, J. J. T. Hogh, APPL. OPTICS, Vol 17, No 15, 1978, p 2369.

28. Z. B. Alfassi, M. Baer, IEEE J. QUANTUM ELECTRON., QE-15, No 4, 1979, p 240.

29. N. G. Basov, A. S. Bashkin, P. G. Grigor'yev et al., KVANTOVAYA ELEKTRONIKA, Vol 3, No 9, 1976, p 2067.

30. A. S. Bashkin, A. N. Orayevskiy, V. N. Tomashov, N. N. Yuryshev, KVANTOVAYA ELEKTRONIKA, Vol 7, 1980, p 1357.

31. A. S. Bashkin, N. P. Vagin, O. R. Nazyrov et al., KVANTOVAYA ELEKTRONIKA, Vol 7, No 8, 1980.

32. A. S. Bashkin, A. F. Konoshenko, A. N. Orayevskiy et al., KVANTOVAYA ELEKTRONIKA, Vol 5, No 7, 1978, p 1608.

33. J. A. Mangano, R. L. Limpaecher, J. D. Daugherty, F. Russel, APPL. PHYS. LETTS, Vol 25, No 5, 1975, p 293.

34. R. A. Gerber, E. L. Patterson, L. S. Blair, N. R. Greiner, APPL. PHYS. LETTS, Vol 25, No 5, 1974, p 281.

35. D. B. Nichols, R. B. Hall, J. D. McClure, J. APPL. PHYS., Vol 47, No 9, 1976, p 4026.

36. V. I. Igoshin, V. Yu. Nikitin, A. N. Orayevskiy, KRATKIYE SOOBSHCHENIYA PO FIZIKE, FIAN, No 26, 1978, p 20.

37. V. N. Kondrat'yev, Ye. Ye. Nikitin, "Kinetika i mekhanizm gazofaznykh reaktsiy" [Kinetics and Mechanism of Gas-Phase Reactions], Moscow, Nauka, 1974, p 443.

38. N. N. Semenov, "O nekotorykh problemakh khimicheskoy kinetiki i reaktsionnoy sposobnosti" [Concerning Some Problems of Chemical Kinetics and Reactivity], USSR Academy of Sciences, Moscow, 1958.

39. G. K. Vasil'yev, Ye. F. Makarov, Yu. A. Chernyshev, DOKLADY AKADEMII NAUK SSSR, Vol 233, 1977, p 1118.

40. V. I. Igoshin, V. Yu. Nikitin, A. N. Orayevskiy, KVANTOVAYA ELEKTRONIKA, Vol 7, No 7, 1979.

41. N. G. Basov, Ye. P. Markin, A. N. Orayevskiy, A. V. Pankratov, DOKLADY AKADEMII NAUK SSSR, Vol 198, No 5, 1971, p 1043.

42. V. I. Igoshin, A. N. Orayevskiy, KVANTOVAYA ELEKTRONIKA, Vol 6, No 12, 1979, p 1912.

43. N. L. Kupriyanov, Dissertation, Physics Institute imeni P. N. Lebedev, USSR Academy of Sciences, Moscow, 1979.

44. A. S. Bashkin, N. L. Kupriyanov, A. N. Orayevskiy, KVANTOVAYA ELEKTRONIKA, Vol 5, No 12, 1978, p 2611.

45. V. A. Danilychev, O. M. Kerimov, I. B. Kovsh, TRUDY FIZICHESKOGO INSTITUTA IMENI P. N. LEBEDEVA, AKADEMII NAUK SSSR, Vol 85, 1976, p 49.

46. I. S. Datskevich, V. S. Zuyev, L. D. Mikheyev, I. V. Pogorel'skiy, KVANTOVAYA ELEKTRONIKA, Vol 5, 1978, p 1456.

47. A. N. Oraevsky, "Chemical Lasers: Present Situation and Trends," Preprint FIAN, No 88, 1977.

[8144/0285-6610]

6610
CSO: 8144/0285

UDC 621.375.8

ABSTRACTS FROM THE COLLECTION 'OPTICALLY PUMPED GAS LASERS'

Moscow GAZOVYYE LAZERY S OPTICHEKOY NAKACHKOY [TRUDY ORDENA LENINA FIZICHESKOGO INSTITUTA IMENI P. N. LEBEDEVA ADAKEMII NAUK SSSR] in Russian Vol 125, 1980 pp 2, 218, 219

[Text] This collection presents the results of experimental and theoretical research done in the Quantum Radio Physics Laboratory on the following major problems: photolysis of gaseous compounds that contain bonds between the iodine atom and elements of the fourth and fifth groups of the periodic table with discussion of potential applications of the results to development of a recombination version of the iodine laser and to separation of iodine isotopes; principles of forming, amplifying and analyzing powerful nanosecond light pulses by iodine lasers, the parameters of the experimental facility and questions of improving the characteristics of the output emission; the working principle of a cooled photochemical XeO laser with pumping by the emission from a high-current open electric discharge, and the outlook for further improving the output characteristics of such a laser; lasing by vapors of complex chemical compounds, and the prospects for using them as active media in lasers with incoherent optical pumping; the vibrational structure of the laser transition $B^2\Sigma^+_{1/2} - X^2\Sigma^+_{1/2}$ of the XeF molecule.

The publication is aimed at a broad class of scientists and engineers specializing in the field of quantum radio physics.

UDC 621.375.826+535.342+535.372

LASING BY XeF WITH OPTICAL PUMPING, AND ANALYSIS OF THE SPECTRUM OF THE LASER TRANSITION $B^2\Sigma^+_{1/2}-X^2\Sigma^+_{1/2}$

[Abstract of article by Zuyev, V. S., Kanayev, A. V., Mikheyev, L. D. and Stavrovskiy, D. B.]

[Text] The paper discusses the working principle of a photochemical XeF laser ($\lambda \approx 350$ nm). A laser is described that operates with pumping of the XeF_2:$N_2(SF_6)$:Ar gas mixture by radiation from an open high-current discharge. Maximum lasing duration was 5 μs, and maximum output energy was 0.15 J. An investigation was made of the vibrational structure of the $B^2\Sigma^+_{1/2}-X^2\Sigma^+_{1/2}$ transition as observed in the XeF molecule in absorption, luminescence and stimulated emission. The vibrational quantum and anharmonicity were measured in the upper and lower states: $\omega'_e = 308.7$ cm^{-1}, $\omega'_e x'_e = 1.44$ cm^{-1}, $\omega''_e = 225.7$ cm^{-1}, $\omega''_e x''_e = 11.0$ cm^{-1}. The difference between equilibrium internuclear distances of the XeF molecule is determined for the excited (B) and ground (X) states: $r''_e - r'_e = 0.33 \pm 0.01$ Å. Figures 12, references 63.

UDC 621.373.8

LASERS THAT USE VAPORS OF COMPLEX ORGANIC COMPOUNDS

[Abstract of article by Zuyev, V. S., Stoylov, Yu. Yu. and Trusov, K. K.]

[Text] A theoretical examination is made of the emission characteristics of lasers based on complex organic compounds in the quasi-steady state with consideration of induced losses in the spectral region of lasing in a system of triplet and excited singlet states of the molecules. The results of the calculations are compared with experimental data for POPOP and TOPOT vapor lasers. An investigation is made of the thermal stability of these compounds at $T < 600$ K. The singlet-triplet conversion constants and absorption cross sections of excited singlet molecules of TOPOT in the lasing band were determined, and the effectiveness of using a buffer gas to stabilize POPOP and TOPOT molecules was estimated. Figures 11, references 67.

UDC 621.378.8

EMISSION AND AMPLIFICATION OF NANOSECOND PULSES BY IODINE LASERS

[Abstract of article by Zuyev, V. S., Katulin, V. A., Nosach, V. Yu. and Petrov, A. L.]

[Text] The paper gives the results of experimental research on iodine photolysis high-power lasers with pumping by lamps and by the emission from high-current electric discharges. An investigation is made of the fundamental parameters of the working medium, the parameters of lasers with both lamp pumping and electric discharge pumping, and methods of shaping a short pulse with the directivity of lasing at the diffraction limit. It is demonstrated that it is potentially feasible to amplify a short pulse with an iodine amplifier pumped by a high-current open discharge. An iodine laser is described that produces a pulse with duration of 1 ns, divergence of 10^{-4} radian and energy of 100 J at a constrast of 10^8, and 300 J at a contrast of 10^2-10^3. Figures 37, references 67.

UDC 621.373.8

A XENON OXIDE PHOTOCHEMICAL LASER

[Abstract of article by Zuyev, V. S., Mikheyev, L. D. and Pogorel'skiy, I. V.]

[Text] The paper describes theoretical and experimental research on development, creation and investigation of the peculiarities of a photochemical laser based on xenon oxide, using photodissociation of nitrous oxide by the vacuum ultraviolet emission of an open high-current discharge with formation of oxygen atoms and subsequent oxidation of xenon. An examination is made of the theoretical problems associated with substantiation of the mechanism and calculation of the kinetics of physicochemical processes in the XeO laser. Pumping is numerically analyzed, and inversion and gain on the laser transition are computed. The laser design is described, and also the procedure used in experiments that give optimum temperatures, composition and pressure of components of the working mixture yielding a lasing energy of 2.2 J in a pulse from an active volume of about 1 liter. The spectral

composition of the laser emission and the energy characteristics of the laser are studied. The heat release during photolysis is estimated as well as the rate constants of quenching of the upper laser state of XeO ($2^1\Sigma^+$) and the vibrational relaxation of the lower state of XeO ($1^1\Sigma^+$). A theoretical investigation is made of the internal losses in the active medium of a photochemical XeO laser. An estimate is made of the feasibility of increasing the volume of the active medium by using a plane-parallel cavity. Figures 20, tables 3, references 49.

UDC 621.375.826

INVESTIGATION OF PROCESSES OF PHOTOLYSIS OF COMPOUNDS WITH P-I AND As-I BONDS

[Abstract of article by Andreyeva, T. L., Birich, G. N., Sorokin, V. N., Struk, I. I. and Suvorov, D. N.]

[Text] Detailed experimental studies are done on the parameters of lasing on the transition $^2P_{1/2} \rightarrow {}^2P_{3/2}$, $\lambda = 1.3$ μm of atomic iodine that arises upon photodissociation of molecules of $(CF_3)_2AsI$ and $(CF_3)_2PI$. The light source was an IFP-5000 xenon flashlamp. On the basis of the resultant experimental data, a scheme is devised for the principal reactions that accompany photolysis of molecules of $(CF_3)_2AsI$ and $(CF_3)_2PI$ and that determine the energy parameters of the stimulated emission. Figures 8, table 1, references 18.

UDC 541.14

INVESTIGATION OF PROCESSES OF PHOTODISSOCIATION OF MOLECULES OF $SiCl_3I$ AND SiF_3I

[Abstract of article by Andreyeva, T. L., Sorokin, V. N. and Struk, I. I.]

[Text] Experimental research is done on lasing on a transition of atomic iodine that is stimulated upon photodissociation of molecules of $SiCl_3I$ and SiF_3I. A xenon-filled coaxial flashlamp of original design was used as the light source. An analysis is made of the principal chemical reactions that accompany photolysis of molecules of $SiCl_3I$ and SiF_3I, and that determine the energy characteristics of the stimulated emission. Figures 10, references 10.

UDC 621.375.826

CONCERNING POSSIBILITIES OF [EMISSION] IN THE VISIBLE BAND WITH PHOTODISSOCIATION OF MOLECULES

[Abstract of article by Andreyeva, T. L.]

[Text] An analysis is made of lower excited states of some diatomic radicals and atoms from which transitions to the ground state lie in the visible and near ultraviolet region of the spectrum. An examination is made of possible mechanisms of formation of inversion upon photodissociation of molecules by radiation from a source with continuous spectrum for which the brightness temperature is $T \approx 3 \cdot 10^4$ K. Figure 1, tables 2, references 27.

UDC 621.378.33

REACTIONS OF IODINE ATOMS IN THE EXCITED [I* ($^2P_{1/2}$)] AND UNEXCITED [I ($^2P_{3/2}$)] STATES WITH PERFLUOROALKYL RADICALS

[Abstract of article by Andreyeva, T. L., Kuznetsova, S. V., Maslov, A. I. and Sobel'man, I. I.]

[Text] A method of studying reactions of excited and unexcited atoms is discussed that is based on flash photolysis of molecules with simultaneous transillumination of the working medium by resonant laser emission. The proposed technique is used for studying reactions that accompany photolysis of molecules of RI (CF_3I, p-C_3F_7I, i-C_3F_7I). Rate constants are determined for recombination of iodine atoms into I_2 in the presence of RI molecules for atoms of I ($^2P_{3/2}$) and I* ($^2P_{1/2}$), as well as the constants for recombination of radicals R into R_2, and for recombination of radicals R with atoms of I* ($^2P_{1/2}$) and I ($^2P_{3/2}$) into the RI molecule. It is shown that in reactions of recombination into I_2 and RI, atoms of I ($^2P_{3/2}$) are much more active than atoms of I* ($^2P_{1/2}$). The authors discuss the part played by the investigated reactions in the kinetics of the flash photolysis laser. Results are compared with data in the literature. Figures 4, tables 7, references 43.

UDC 621.378.833

ON THE POSSIBILITY OF USING RECOMBINATION REACTIONS AND ALKALI METALS TO GET POPULATION INVERSION ON ATOMIC IODINE

[Abstract of article by Andreyeva, T. L., Babkin, V. I., Maslov, A. I., Sobel'man, I. I. and Yukov, Ye. A.]

[Text] The authors consider the feasibility of developing a continuous-flow version of a laser using a transition of atomic iodine. Population inversion arises as a result of depletion of the lower laser level due to preferred recombination of iodine atoms in the ground state into molecules. Atoms of alkali metals are used to get atomic iodine and free radicals without expending electric energy. It is proposed that an electric discharge be used for exciting the atomic iodine. An examination is made of the kinetics of the principal chemical reactions, and the possibility of achieving inversion is demonstrated for reasonable parameters of the working medium. A schematic diagram of the laser facility is discussed. Figures 3, tables 2, references 14.

UDC 621.039.335+621.378.33

INVESTIGATION OF THE FEASIBILITY OF SEPARATING ISOTOPES ^{127}I AND ^{129}I BY AN IODINE PHOTODISSOCIATION LASER

[Abstract of article by Andreyeva, T. L., Kuznetsova, S. V., Maslov, A. I., Sobel'man, I. I. and Yukov, Ye. A.]

[Text] A method of separating iodine isotopes is proposed that is based on the considerable difference of the rate constants of reactions of excited I* ($^2P_{1/2}$) and

unexcited iodine atoms with CF_3 radicals and Cl_2 molecules, and on the possibility of using an iodine photolysis laser based on $R^{127}I$ molecules ($\lambda = 1.315$ μm) to act on ^{127}I atoms in states $^2P_{1/2}$ and $^2P_{3/2}$. An investigation is made of the feasibility of isolating the pure ^{129}I isotope and a mixture of ^{127}I and ^{129}I. Figures 6, table 1, references 14.

6610
CSO: 1862

UDC 621.373.826

A PULSE-PERIODIC PHOTODISSOCIATIVE IODINE LASER PUMPED BY THE RADIATION OF MAGNETOPLASMA COMPRESSORS

Moscow KVANTOVAYA ELEKTRONIKA in Russian Vol 7, No 9(99), Sep 80 pp 2052-2054 manuscript received 13 Mar 80

[Article by G. N. Kashnikov, V. K. Orlov, A. N. Panin, A. K. Piskunov and V. A. Reznikov]

[Text] The authors study the characteristics of a photodissociative iodine laser pumped by magnetoplasma compressor emission. The laser design uses a system of closed circulation of the C_3F_7I working gas. A pulse-periodic operating mode is realized with an interval of 1 minute between pulses, a lasing energy level of 110 J and pulse duration of 30 μs.

In designs of photodissociative iodine lasers developed for nuclear fusion facilities, the optical pumping source is either an open electric discharge [Ref. 1] or xenon lamps that operate in the brief flash mode with duration of a few dozen microseconds [Ref. 2]. In this type of excitation, the amplifying medium does not contain shock waves that produce optical inhomogeneities and considerably increase the divergence of radiation at the output of the amplifier. To produce short electric supply pulses in these cases we must produce a voltage surge across discharge gaps 0.5-1 m long, which requires the development of high-voltage ($U \geqslant 50$ kV) and commutating devices.

The use of quartz optical pumping sources based on magnetoplasma compressors [Ref. 3] avoids these difficulties since the power supply in the short pulse mode is a low-voltage battery ($U = 3$-5 kV), and discharge initiation (creeping discharge over a surface a few centimeters long) is by a trigatron circuit where synchronous operation of any number of sources does not require commutators. By using such sources in addition to lamps a system for closed circulation of the working mixture can be realized in iodine lasers [Ref. 2], which considerably reduces the expenditure of working gases when the laser is operated in the pulse-periodic mode.

The photodissociative laser studied here consists of a working chamber with five pumping sources based on magnetoplasma compressors perpendicular to the optical axis in the middle plane of the reactor. The quartz container of each source is 50 mm in diameter. The chamber measures 1000 x 250 x 250 mm; it is equipped with an optical window measuring 250 x 250 mm. Each compressor is supplied by an independent capacitor bank with capacitance of 800 μF charged to 3.3 kV, discharge half-period

is $\tau_2 = 26$ μs, the attenuation constant of the loop is $P = 4 \cdot 10^4$ s^{-1}. The coefficient of transfer of the energy stored in the loop to the plasma is 0.8. Discharges of the magnetoplasma compressor were triggered by an ignition pulse (τ_i = 2 μs, $E_i = 1$ J) with electrical separation into ten channels; the spread in firing of discharges was about 1 μs. Structurally, the cavities of the pumping sources were interconnected, and removal of products of erosion was done by a vacuum pump down to a pressure of about $5 \cdot 10^{-2}$ mm Hg. The electric power supply system can give discharges at a level of $E_{st} = 36$ kJ once per minute. Attached to the reactor is a system for closed circulation of the working mixture, shown schematically in Fig. 1. This is made up of a flat cryostat installed in the working gas flow. The cryostat has a recess at the top for liquid phase of the working substance. The circulating blower, based on an induction motor, is located inside of the working space.

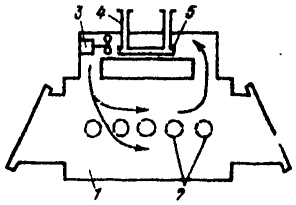

Fig. 1. Diagram of system for closed circulation of the working fluid: 1--working space; 2--optical pumping source based on magnetoplasma compressor; 3--circulating blower; 4--cryostat; 5--liquid phase of C_3F_7I

The working fluid was p-C_3F_7I diluted with SF_6.

The reflectivities of the mirrors in the flat laser cavity were $R_1 = 99\%$, $R_2 = 50\%$, diameter 280 mm. Laser emission was directed by a lens with focal length of 1 m and a reflecting plate to a TPI-2-5 calorimeter. Oscillograms of the emission pulses were recorded by an FD9E111 photodiode.

The maximum emission energy of the laser was $E_e = 115$ J for stored energy in the capacitors of 36 kJ, p-C_3F_7I pressure of 11 mm Hg and 10x dilution with SF_6. The efficiency of the facility was 0.29%, which is close to that of 0.25% achieved previously on an iodine laser pumped with an open discharge at the same stored energy level [Ref. 4].

With an increase in the length of the active region and improvement of the energy parameters of the given type of laser as losses to the lasing threshold are reduced, there is a concomitant improvement in the laser parameters (efficiency of 1 and 1.4% with respect to invested energy in Ref. 1 and 5 respectively). Upon repeated initiation of the same mixture the lasing energy decreases due to buildup of the molecular iodine and reduction in the pressure of the working component (Fig. 2, curve 1). The idea behind the system for closed circulation of the working

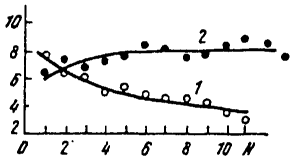

Fig. 2. Lasing energy as a function of the number of pulses without replacement of the working fluid: $P_{C_3F_7I} = 11$ mm Hg, $P_{SF_6} = 110$ mm Hg (1) and with the use of a closed circulating system, $P_{SF_6} = 110$ mm Hg (2)

fluid is removal of the I_2 by freezing it out on a cooled surface, and restoration of the pressure of the working component to the equilibrium level by evaporating the p-C_3F_7I from the liquid phase [Ref. 6].

An experiment with use of the closed circulating system was done in the following arrangement. The working gas was let into the reactor to a pressure of 30 mm Hg, the cryostat was cooled to -50°C, which corresponds to a p-C_3F_7I pressure of 10 mm Hg, and then SF_6 was added to a pressure of 100 mm Hg and the closed circulating system was switched on. The mixture was optically stimulated at a rate of once per minute at $E_{st} = 36$ J. Up to the fifth pulse the optimum pressure of the working component was determined by variation of the cold trap temperature, and then the temperature was stabilized at -40°C, which corresponds to a pressure of $P_{C_3F_7I} = 23$ mm Hg. The lasing energy in subsequent pulses was stable: $E_e = 110$ J (Fig. 2, curve 2). It should be noted that at such a C_3F_7I pressure, pumping emission losses due to vignetting by the quartz sources amounted to about 1/3. Fig. 3 shows oscillograms of lasing pulses recorded in two sections of the semitransparent mirror. Close to the surface of the pumping sources the lasing pulse shape (Fig. 3b) differed considerably from the pumping pulse shape. Close to the wall of the reactor, the lasing pulse shape (Fig. 3c) repeated the pumping pulse. No interruption of lasing due to pyrolysis was observed over the entire end face of the laser.

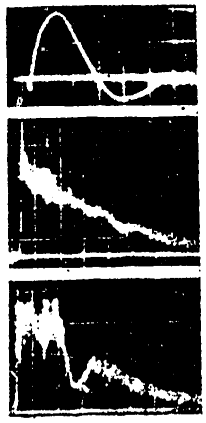

Fig. 3. Oscillograms of magnetoplasma compressor current pulses (a), lasing pulses at the surface of the pumping sources (b) and in the midsection of the space between the sources and the reactor wall (c); $P_{C_3F_7I} = 11$ mm Hg, $P_{SF_6} = 110$ mm Hg, scale 10 μs/div

The proposed laser can be used as a signal amplifier for a master Q-switched laser. For spectral matching of the signals of the master laser and amplifier, a method can be used that provides for delivering the signal of the master laser at zero current of the magnetoplasma compressor of the amplifier [Ref. 1] when the magnetic field in the amplifier space is minimum and displacement of the amplification line is insignificant.

REFERENCES

1. V. A. Katulin, V. Yu. Nosach, A. L. Petrov, KVANTOVAYA ELEKTRONIKA, Vol 3, 1976, p 1829.

2. G. Bredlov, Ye. Fill, V. Fuse, K. Fola, R. Fol'k, Ye. Vitte, KVANTOVAYA ELEKTRONIKA, Vol 3, 1976, p 906.

3. A. S. Kamrukov, G. N. Kashnikov, N. P. Kozlov, V. K. Orlov, Yu. S. Protasov, PIS'MA V ZHURNAL TEKHNICHESKOY FIZIKI, Vol 3, 1977, p 2334.

4. N. G. Basov, L. Ye. Golubev, V. S. Zuyev, V. A. Katulin, V. N. Netemin, O. Yu. Nosach, V. Yu. Nosach, A. L. Petrov, KVANTOVAYA ELEKTRONIKA, No 6, 1973, p 116.

5. I. L. Yachnev, Author's abstract of candidate's dissertation, Leningrad, State Optics Institute, 1978.

6. W. Fuss, K. Hohla, OPTICS COMMS, Vol 18, 1976, p 427.

6610
CSO: 1862

UDC 621.373.8

CONCERNING THE CHANGE IN SHIELDING ACTION OF PRODUCTS OF THERMAL DISSOCIATION OF MATERIALS UNDER THE EFFECT OF LASER EMISSION IN A MOVING MEDIUM

Moscow KVANTOVAYA ELEKTRONIKA in Russian Vol 7, No 9(99), Sep 80 pp 2049-2051 manuscript received 3 Mar 80

[Article by N. A. Kirichenko, A. G. Korepanov and B. S. Luk'yanchuk, Physics Institute imeni P. N. Lebedev, USSR Academy of Sciences, Moscow]

[Text] The paper discusses the feasibility of reducing the strong shielding action of products of combustion of organic materials produced by CO_2 laser emission by entrainment of dispersed carbon in a gas stream under the action of a blast through the radiation-affected zone.

Products of combustion of organic materials (soot particles, CO_2 molecules and so on) strongly absorb radiation with $\lambda = 10.6$ μm. This phenomenon leads to increased energy inputs when CO_2 laser radiation is used to treat such materials as wood, textolite and the like. In this connection it is of interest to study the feasibility of reducing the screening action of combustion products by a blast through the radiation-affected zone.

In the general case, the problem of combustion is quite complicated since it is necessary to take consideration of a number of factors such as the energy released during burning, heat exchange with the medium and so on. In this paper we consider a simpler problem where the exothermal reaction can be disregarded. Such a situation may arise for example with thermal dissociation of organic molecules in an inert atmosphere under the effect of laser emission, or if the intensity of radiation is great compared with the intensity of energy released by the reaction itself.

In the case of thermal dissociation of organic materials in an inert atmosphere [Ref. 1], one of the major products of the process is dispersed carbon (soot). Therefore let us assume for the sake of simplicity that the screening action of the products of dissociation is due entirely to dispersed carbon. In blasting, the soot particles are entrained by the gas flow, which changes the screening action.

The influence that cross blasting the radiation-affected zone has on the effectiveness of laser heating of metals was studied in Ref. 2-4. However, these papers considered the mechanical action of a stream of gases leading to the formation and entrainment of liquid metal droplets due to the development of hydrodynamic

instabilities in a layer of melt. The transverse movement of the stream produced a greater rate of removal of material than in the case of direct vaporization since part of the laser radiation energy was not expended on the latent heat of vaporization. However, effects associated with a change in screening of the surface of the material by products of laser destruction were not considered in Ref. 2-4. At the same time, we know that the screening action of such products may be considerable [Ref. 5, 6].

Consider the following model of the investigated effect. Assume that CO_2 laser radiation flux with uniform distribution of intensity over the cross section of a beam of radius a is incident on the material of a target that occupies the half-space $z \leqslant 0$. The target is blasted by a gas flow with velocity v directed parallel to the surface. As shown by simple estimates using a method outlined in Ref. 6, for the parameters of the problem that are interest to us, the dimensions of soot particles R_0 are usually $\sim 10^{-6}$ cm [Ref. 1, 7, 8], and in times of the order of $\tau \ll a/v$ the temperatures and velocities of the particles and those of the gas flow become equal. Thereafter, the spatial distribution of soot particles changes as a result of diffusion in the moving gas. In an approximation that assumes that the sizes of all particles are the same (the actual size distribution of particles is given in Ref. 1) and that their concentration is fairly small, the problem is described by by a system of equations of diffusion of particles in the gas and thermal conductivity in the target material

$$\begin{cases} D\,\Delta n - v\,\dfrac{\partial n}{\partial x} = 0, \quad x = r\cos\varphi, \quad z \geqslant 0, \\ -D\,\dfrac{\partial n}{\partial z}\Big|_{z=0} = Q(r, \varphi), \end{cases} \tag{1}$$

$$\begin{cases} \Delta T = 0, z \leqslant 0, \\ k\,\dfrac{\partial T}{\partial z}\Big|_{z=0} = \begin{cases} I(r, \varphi) - \eta\,(T|_{z=0} - T_\infty), & r \leqslant a, \\ -\eta\,(T|_{z=0} - T_\infty), & r > a, \end{cases} \end{cases} \tag{2}$$

$$I(r, \varphi) = I_0 \exp\left\{-\sigma \int_0^\infty n(r, \varphi, z)\,dz\right\} \theta(a - r). \tag{3}$$

Here r, ϕ, z are cylindrical coordinates; $D = k_B T_\infty / 6\pi\mu R_0$ is the coefficient of Brownian movement of the soot particles; T_∞ is the temperature of the gas stream; μ is the coefficient of dynamic viscosity of the gas; k is the coefficient of thermal conductivity of the material; I_0 is the initial flux density of the radiation (as $z \to \infty$).

The flux density of particles of soot leaving the surface is given with reasonable accuracy by the expression [Ref. 9]

$$Q = N\frac{\bar{c}}{4x_0}\,\frac{\alpha}{k_B T}\exp\left(-\frac{\alpha}{k_B T}\right), \tag{4}$$

where $N = \frac{1}{4R_0^2}$ is the surface concentration of soot particles; $\bar{c} = (8k_B T/\pi m)^{1/2}$ is the average thermal velocity of the particles, corresponding to surface temperature T; $\alpha = A_0 \frac{\rho}{\rho_0}\,\frac{0}{6x_0}$; ρ is the density of the material; $\rho_0 = 2.25$ g/cm^3 is the density of graphite; $A_0 = 46.9 \cdot 10^{-13}$ erg; $x_0 = 4 \cdot 10^{-8}$ cm are material constants [Ref. 10].

The cross section of radiation absorption by a small particle ($2\pi R_0/\lambda \ll 1$) is given by the Mie formula [Ref. 11]:

$$\sigma = 8\pi^3 R_0^3 \lambda^{-1} \operatorname{Im}[(\varepsilon-1)/(\varepsilon+2)], \tag{5}$$

where $\varepsilon = (3.48 + 2.46i)^2$ is the permittivity of soot on a wavelength of 10.6 μm [Ref. 12].

The coefficient of heat exchange η between the target and the moving gas stream can be written as the sum of coefficients of molecular [Ref. 13] and convective [Ref. 14] heat exchange:

$$\eta = \frac{1}{\sqrt{2\pi}} \rho_T \frac{R}{A} \sqrt{\frac{RT_\infty}{A}} + 0{,}332 \frac{\varkappa}{L} \sqrt{\mathrm{Re}_0}\, \mathrm{Pr}^{1/3}. \tag{6}$$

Here ρ_T is gas density; R is the universal gas constant; A is atomic weight; κ is the coefficient of thermal conductivity of the gas; $\mathrm{Re} = vL/\nu$ is the Reynolds number of the gas stream; $\mathrm{Pr} = \nu/\chi$ is the Prandtl number; ν is the coefficient of kinematic viscosity of the gas; χ is the coefficient of thermal diffusivity of the gas; L is the distance from the edge of the plate to the point where η is calculated (if $a \ll L$, η is independent of the coordinates in the region of interest to us).

By using finite Fourier transformation with respect to ϕ, Hankel transformation with respect to r and Fourier transformation with respect to z, system of equations (1)-(3) can be reduced to a system of integral equations:

$$\begin{aligned} \bar{T} &= \exp\left\{ -\frac{\sigma Q_0 a^2}{D} \int_0^\infty \bar{r}_1 d\bar{r}_1 \int_0^{2\pi} \frac{d\varphi_1}{2\pi} \exp\left[\frac{va}{2D} (\bar{r}\cos\varphi - \bar{r}_1 \cos\varphi_1) \right] \times \right. \\ &\qquad \left. \times K_0\left(\frac{va}{2D} u\right) \bar{Q}(\bar{r}_1, \varphi_1) \right\}, \\ \bar{T} &= \int_0^1 \bar{r}_1 d\bar{r}_1 \int_0^{2\pi} \frac{d\varphi_1}{2\pi} \bar{I}(\bar{r}_1, \varphi_1) \left\{ \frac{1}{u} - \frac{\pi}{2} \frac{\eta a}{k} \left[H_0\left(\frac{\eta a}{k} u\right) - N_0\left(\frac{\eta a}{k} u\right) \right] \right\} + \bar{T}_\infty. \end{aligned} \tag{7}$$

Here we use the following notation: $\bar{r} = r/a$; $\bar{T} = T/T_0$; $\bar{I} = I/I_0$; $T_0 = aI_0/k$; $\bar{T}_\infty = T_\infty/T_0$; $\bar{Q} = Q/Q_0$; $Q_0 = Q(T - T_0)$; $u = [\bar{r}^2 + \bar{r}_1^2 - 2\bar{r}\bar{r}_1 \cos(\phi - \phi_2)]^{1/2}$; K_0 is the cylindrical function of the imaginary argument; H_0 is the Struve function; N_0 is the Neumann function [Ref. 15].

System of equations (7) was numerically solved on a computer by a method of sucessive iterations for values of the parameters $a/k_B T = 10$; $T_\infty/T_0 = 0.1$. Fig. 1 shows how the emission power that reaches the surface through the absorbing layer of soot particles depends on the velocity of the blast without consideration of heat exchange, i. e. at $\eta a/k = 0$ and $\sigma Q_0 a^2/D = 10^4$ (curve 1), 10^6 (2), 10^8 (3) and 10^{10} (4). The stream is completely blown away when $va/2D \sim 10^7$, which corresponds to a gas flow velocity $v \approx 2$ m/s (for particles with a size of $R_0 = 10^{-6}$ cm, $a = 1$ cm).

Fig. 2 illustrates the influence of heat exchange on the surface. The radiation power that reaches the surface of the target is plotted as a function of the heat

exchange parameter $\eta a/k$ for $va/2D = 10^3$ and for the same values of the absorption parameter $\sigma Q_0 a^2/D$ as in Fig. 1.

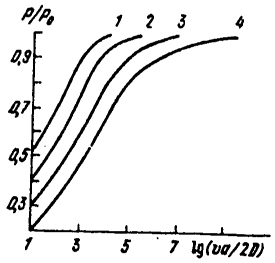

Fig. 1

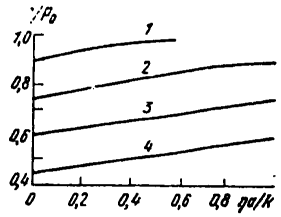

Fig. 2

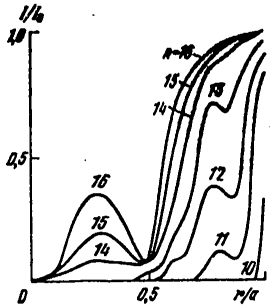

Fig. 3

Shown in Fig. 3 at $va/2D = 10$, $\sigma Q_0 a^2/D = 10^{10}$, $\eta a/k = 0$ is the typical distribution of radiation flux density with respect to radii of the zone of exposure that make angles $\phi = n\pi/16$ with the velocity vector of the gas stream. For angles $\phi < 10\pi/16$ the penetrating flux is nearly zero practically everywhere except in the vicinity of the beam boundary $r = a$, and is not indicated on Fig. 3.

These results imply that although the integrated radiation flux reaching the surface of the target changes monotonically with increasing velocity of the blast (see Fig. 1), the spatial distribution of intensity is nevertheless quite complicated in structure, and does not reduce to monotonic behavior along the direction of the blast. We note that it is typical for such structures to arise in problems described by a system of coupled diffusion equations [Ref. 16]. Experimental verification of such peculiarities of heating of matter is of interest in this connection.

The authors thank F. V. Bunkin for useful discussion of this work.

REFERENCES

1. A. N. Il'in, E. I. Tsygankova et al., in: "Puti razvitiya promyshlennosti tekhnicheskogo ugleroda" [Paths of Development of the Technical Carbon Industry], Moscow, Scientific Research Institute of the Tire Industry, 1978, p 28; V. F. Surovikin et al., Ibid., p 102.

2. R. L. Johnson, J. D. O'Keefe, AIAA J., Vol 12, 1974, p 1106.

3. J. Robin, P. Nordin, J. APPL. PHYS., Vol 46, 1975, p 2538.

4. J. E. Robin, P. Nordin, APPL. PHYS. LETTS, Vol 26, 1975, p 289.

5. V. D. Lokhnygin, A. A. Samokhin, PIS'MA V ZHURNAL TEKHNICHESKOY FIZIKI, Vol 1, 1975, p 749.

6. S. I. Anisimov, Ya. I. Imas, G. S. Romanov, Yu. V. Khodyko, "Deystviye izlucheniya bol'shoy moshchnosti na metally" [Effect of High-Power Radiation on Metals], Moscow, Nauka, 1970.

7. A. J. Medalia, F. A. Heckman, CARBON, Vol 7, 1969, p 567.

8. A. J. Medalia, Z. W. Richards, J. COLLOID AND INTERFACE SCI., Vol 40, 1972, p 233.

9. B. Dahneke, J. COLLOID AND INTERFACE SCI., Vol 50, 1975, p 89.

10. B. Dahneke, J. COLLOID AND INTERFACE SCI., Vol 40, 1972, p 1.

11. R. Newton, "Teoriya rasseyaniya voln i chastits" [Theory of Scattering of Waves and Particles], Moscow, Mir, 1969.

12. R. Siegel, J. Howell, "Teploobmen izlucheniyem" [Heat Exchange by Radiation], Moscow, Mir, 1975.

13. G. N. Patterson, "Molekulyarnoye techeniye gazov" [Molecular Flow of Gases], Moscow, Fizmatgiz, 1960.

14. J. E. Meyers, K. O. Bennet, "Gidrodinamika, teploobmen i massoobmen" [Hydrodynamics, Heat Exchange and Mass Exchange], Moscow, Nedra, 1966.

15. I. S. Gradshteyn, I. M. Ryzhik, "Tablitsy integralov, summ, ryadov i proizvedeniy" [Tables of Integrals, Sums, Series and Products], Moscow, Nauka, 1962.

16. V. A. Vasil'yev, Yu. M. Romanovskiy, V. G. Yakhno, USPEKHI FIZICHESKIKH NAUK, Vol 125, 1979, p 625.

[13-6610]

6610
CSO: 1862

UDC 621.373.826.038.823

PUMPING OF ELECTRON BEAM-CONTROLLED CO_2 LASERS WITH MAXIMUM BEAM UTILIZATION FACTOR

Moscow KVANTOVAYA ELEKTRONIKA in Russian Vol 7 No 9(99) Sep 80 pp 1979-1984 manuscript received 28 Jun 79, after revision 24 Jun 80

[Article by A. I. Avrov, Ye. P. Glotov, V. A. Danilychev and N. V. Cheburkin, Physics Institute imeni P. N. Lebedev, USSR Academy of Sciences, Moscow]

[Text] The excitation pulse parameters of electron beam-controlled CO_2 lasers are comprehensively optimized to maximize the beam utilization factor. The optimum pumping pulse duration and laser cavity transmittance are calculated, as well as the optimum specific energy input. It is shown that under optimum conditions at field strengths that do not exceed the threshold of streamer breakdown of the discharge gap, a high beam utilization factor of $\xi = 200$-300 is realized, i. e. the lasing energy Q is 200-300 times the energy expended on ionizing the laser mixture.

Of considerable current interest are cw [Ref. 1] and pulse-periodic [Ref. 2] electron beam-controlled CO_2 lasers in which the maximum average lasing power depends on a large number of parameters such as the lasing mixture circulation rate (gas flowrate), power of the main discharge supply source, maximum radiation load on the mirrors, which determines beam aperture, maximum average current density of ionizing electrons, which is determined by overheating of the separative foil of the electron guns, and so on. The optimum mode of excitation of pulse-periodic electron beam-controlled lasers differs depending on which of these parameters limits the maximum average lasing power. When the power of the supply source is limited, the optimum mode is one with maximum efficiency. In the case where the circulating system does not provide the necessary flowrate of the lasing mixture, the optimum mode is one in which energy output per unit volume of the pumped gas is maximized.

In the main, it is overheating of the separative foil of the electron guns that now limits average output emission power of pulse-periodic electron beam-controlled lasers. The maximum average electron beam current density that is realizable in technological laser facilities that operate over a long time period does not exceed 10 $\mu A/cm^2$ [Ref. 1]. When the average electron current density is limited, the optimum pumping mode that maximizes the average emission power of a pulse-periodic electron beam-controlled laser is one that maximizes the beam utilization factor rather than efficiency or specific energy output.

In our work we calculated the pumping pulse parameters of electron beam-controlled lasers that maximize the beam utilization factor ξ, i. e. the ratio of the specific

laser radiation energy Q to the electron beam energy released in a unit volume of the laser mixture:

$$\xi = Q/\gamma\varepsilon \int_0^\tau j_e(t)\,dt, \tag{1}$$

where γ is the number of electron-ion pairs formed per cm of the mean free path of the ionizing electrons; ε is the energy in eV expended on formation of one electron-ion pair; $\int_0^\tau j_e(t)\,dt$ is the charge that passes through a unit of area during the pumping pulse time τ.

The quantity ξ is strongly dependent on the composition of the laser mixture. In connection with the fact that carbon dioxide molecules are electronegative, the electron beam utilization factor is low in mixtures with a large CO_2 content. Therefore in the working mixtures of pulse-periodic lasers the fraction of carbon dioxide should be reduced by replacement with nitrogen and helium. Helium is necessary for more effective depopulation of level 01'0, which has a relaxation time in helium 16 times as short as in CO_2 [Ref. 3]. However, the presence of helium leads to a considerable reduction of the streamer breakdown voltage of the discharge gap, and therefore the helium content in the mixture should not be too high. Nor should the ratio of concentrations of N_2 and CO_2 $m = [N_2]/[CO_2]$ be very large since the threshold pumping energy increases in proportion to $(m+1)$. Thus there is an optimum laser mixture composition at which the electron beam utilization factor reaches a maximum. However, at present the optimum composition cannot be theoretically determined because of inadequate investigation of the way that the streamer breakdown voltage and effective rate constants of sticking and recombination of electrons depend on the composition of the laser mixture. We will limit ourselves to a mixture of $CO_2:N_2:He = 1:5:4$, which has been studied in the greatest detail both experimentally [Ref. 4] and theoretically [Ref. 5], and is apparently close to the optimum from the standpoint of electron beam utilization.

In Ref. 3, 6 a universal method was developed for calculating the emission parameters of electron beam-controlled lasers based on numerical solution of rate-constant equations with consideration of all important processes occurring during laser operation. In the case where pumping pulse duration is much longer than the characteristic time of energy transfer from N_2 to CO_2, the relaxation time of the lower vibrational level 01'0 of the CO_2 molecule τ_3 and the lifetime of the upper laser level 00°1 as determined by induced radiation and VT-relaxation, the lasing pulse parameters are defined with adequate accuracy by analytical expressions, and efficiency η is determined from the formula

$$\eta = \eta_{KB} \cdot \eta_B \cdot \eta_p \left(1 - \frac{W_*(T_\tau)}{W}\right) \frac{1}{\tau} \int_0^\tau \left(1 - \frac{w_*(t)}{w(t)}\right) dt, \tag{2}$$

where η_{KB}, η_B and η_p are the quantum efficiency, the integrated efficiency of excitation of level 00°1 of CO_2 and the lower vibrational level of nitrogen as determined by the composition of the gas mixture and the reduced electric field strength E/p [Ref. 5]; $\eta_p = T_p/[T_p + \delta(2-T_p)]$ is the efficiency of the laser cavity as determined by the quality of the mirrors (T_p is the transmittance of the cavity, δ is

the losses on the mirrors); w(t) is the specific pumping power; ε is the excitation energy of the upper laser level; τ is pumping pulse duration;

$$W_*(T_\tau) = \varepsilon_1 (m+1)\left[\frac{\ln(1-T_p-\delta)^{-1}}{2L\sigma(T_\tau)} - qe^{-\varepsilon_0/kT_\tau}[CO_2]\right]$$

is the threshold pumping energy corresponding to the temperature T_τ of the laser mixture at the end of the excitation pulse;

$$q = \frac{B_2}{B_1}\exp\left\{\frac{h\nu}{kT}[F(j-1)-F(j)]\right\}; \quad F(j) = B_v(j+1)j;$$

W is specific energy input; j is the rotational quantum number; B_V is the rotational constant; w_* is the power of relaxation losses (threshold pumping power), which increases sharply with rising temperature.

The balance of charged particles in the electroionization discharge is determined by processes of sticking and detachment of electrons and by electron and ion recombination. The electron beam and discharge current densities are related by the expression

$$\frac{j_e\gamma}{e} = \frac{j_p}{v_{др}(E/p)e}\beta + \alpha\frac{j_p^2}{v_{др}^2(E/p)e^2}, \tag{3}$$

where $v_{др}(E/p)$ is electron drift rate; β and α are the effective constants of sticking and recombination of electrons. The expression for the electron beam utilization factor is easily obtained from formulas (2) and (3):

$$\xi = \frac{\eta_{кв}\eta_в\eta_p(1-W_*/W)\int_0^\tau w(t)(1-w_*/w(t))\,dt}{\int_0^\tau \frac{w(t)\varepsilon}{v_{др}(E/p)E}\left(\beta+\alpha\frac{w(t)}{v_{др}(E/p)eE}\right)dt}. \tag{4}$$

Let us determine the optimum parameters of the pumping pulse that correspond to the maximum beam utilization factor in the case where the pulse takes the shape of a rectangle. In this case the expression for ξ becomes

$$\xi = \frac{\eta_{кв}\eta_в(E/p)\eta_p(1-W_*/W)(1-\bar{w}_*(W)\tau/W)Ev_{др}(E/p)}{\varepsilon(\beta+\alpha W/ev_{др}E\tau)}, \tag{5}$$

where $\bar{w}_*(W)$ is the average power of relaxation losses. For given cavity transmittance, laser mixture composition, length of the active region and reduced field strength the beam utilization factor is a function of the specific energy invested in the discharge and pumping pulse duration. Let us note that the beam utilization factor increases sharply with increasing parameter E/p. At large W when $\alpha W/ev_{др}E\tau$ is much greater than β, $\xi \sim \eta_в(E/p)^4$, where $\eta_в$ is an increasing function of field

strength, i. e. in this case ξ increases more strongly than $(E/p)^4$. The expression for the optimum pumping pulse duration is obtained by differentiating formula (5):

$$\tau_{opt} = \frac{\alpha W}{ev_{др} E\beta}\left(\sqrt{1 + \frac{\beta ev_{др} E}{\bar{w}_* \alpha}} - 1\right). \quad (6)$$

Accordingly the expression for optimum pumping power is written as

$$\bar{w}_{opt} = \bar{w}_*\left(1 + \sqrt{1 + \frac{\beta ev_{др} E}{w_* \alpha}}\right). \quad (7)$$

In the case where the sticking rate is small compared with recombination (β is much less than $\alpha\bar{n}_{e*}$; $\bar{n}_{e*} = \bar{w}_*/ev_{др}E$), $w_{opt} = 2\bar{w}_*$, i. e. in the recombination mode the optimum pumping power corresponding to ξ_{max} is only twice the threshold level and corresponds to an efficiency that is half that for operation in the saturated signal mode ($w \gg w_*$). Thus the pumping mode with maximum beam utilization factor differs sharply from the pumping mode with maximum efficiency.

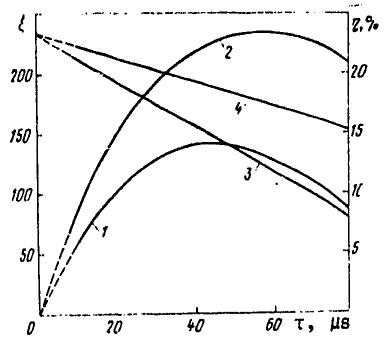

Fig. 1. Electron beam utilization factor ξ (*1*, *2*) and lasing efficiency η (*3*, *4*) as functions of pumping pulse duration for a mixture of CO_2:N_2:He = 1:5:4 at E/p = 4 kV/cm·atm), T_p = 60% and length of the active region L = 2 m; W = 300 (*1*, *3*) and 150 J/(*l*·atm) (*2*, *4*)

Fig. 1 shows theoretical curves for electron beam utilization factor and lasing efficiency as dependent on pumping pulse duration corresponding to different energy inputs. The constants of elementary processes used in the calculations were taken from Ref. 4, 6. The functions $\xi(\tau)$ and $\eta(\tau)$ are qualitatively different: η increases monotonically with increasing τ, and ξ has a maximum. The optimum pumping pulse durations are 55 μs at W = 150 J/(*l*·atm) and 42 μs for W = 300 J/(*l*·atm) (T = 60%, L = 2 m).

The increase in electron beam utilization factor at low τ can be attributed to the fact that the rate of electron loss in the process of dissociative recombination decreases more rapidly with increasing pulse duration than the drop in lasing efficiency. At long durations of the excitation pulse, the rate of electron loss, determined mainly by sticking, is weakly dependent on τ, and the value of ξ drops with increasing pulse duration due to the reduction in efficiency.

To determine how the maximum beam utilization factor depends on W, it is necessary to substitute the expression for optimum pumping pulse duration (6) in formula (5)

$$\xi_{max}(W) = \frac{\eta_{\text{г.н}}\eta_{\text{в}}\eta_{\text{р}}\upsilon_{\text{ид}}E\left[1-\frac{\varepsilon_1(m+1)}{W}\left(\frac{\ln(1-T_p-\delta)^{-1}}{\sigma(T)\,2L}+q\,[CO_2]\,e^{-\varepsilon_1/kT}\right)\right]}{\varepsilon\left[1+(1+\beta/\alpha\bar{n}_{e*})^{1/2}\right]\alpha\bar{n}_{e*}}. \quad (8)$$

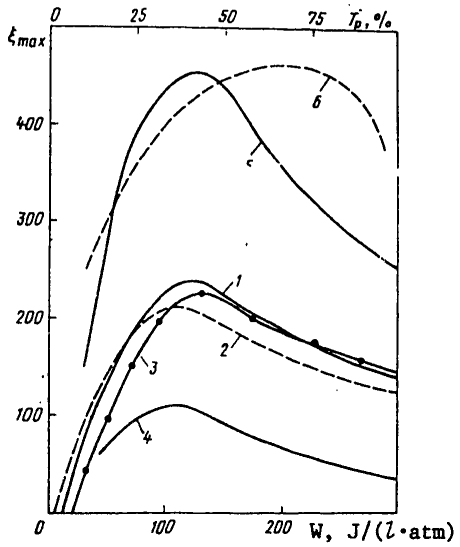

Fig. 2. Maximum electron beam utilization factor as a function of laser cavity transmittance T_p at values of τ and W that are optimum for the given cavity (*6*), and as a function of the specific energy input to the discharge at the optimum pumping pulse duration for the given energy input: E/p = 4 (*1-3*), 3 (*4*) and 5 kV/(cm·atm) (*5*); T_p = 60 (*1*, *4*, *5*), 30 (*2*) and 80% (*3*)

Shown in Fig. 2 are curves for ξ_{max} as a function of the specific energy input for different field strengths and cavity transmittances. We can see that the electron beam utilization factor is a very sharp function of the parameter E/p. At E/p = 5 kV/(cm·atm) (curve 5), ξ_{max} is 4.3 times as high as at E/p = 3 kV/(cm·atm) (curve 4). The optimum energy input in the given range of field strengths depends weakly on E/p, and amounts to 120-140 J/(l·atm). This same figure shows the way that the maximum electron beam utilization factor depends on T_p, corresponding to the optimum pumping pulse duration for each value of cavity transmittance, and to the optimum specific energy input at E/p = 5 kV/(cm·atm) (curve 6). In the calculations the reflectivity of the mirrors was taken as 97% ($\delta = 3(2 - T_p)$%). The function $\xi_{max}(T_p)$ has a smooth maximum at a cavity transmittance of T_p = 65%.

The fact that the maxima of functions $\xi_{max}(W)$ correspond to similar energy inputs at different laser cavity transmittances and field strengths can be attributed to the way that efficiency depends on W. Initially when the threshold is slightly exceeded $\eta_W = (1 - W_*/W)$ and increases sharply with energy input, and then at W of the order of 100 J/(l·atm), η_W reaches a value of about 0.85-0.95 (depending on T_p) and ceases to depend on W (W_* rises in proportion to energy input). At this point the function $\xi_{max}(W)$ reaches a maximum and then begins to fall off since the rate of electron loss due to dissociative recombination rises with increasing discharge current density, which is proportional to W.

At a field strength of $E/p = 4$ kV/(cm·atm), which is easily realized in an electron beam-controlled laser, the maximum value of ξ is 240, i. e. the specific lasing energy is 240 times the energy expended on ionizing a unit of volume of the laser mixture.

Thus the optimization of pumping pulse parameters enables attainment of a very high electron beam utilization factor, which is especially important when an electron beam-controlled laser operates in the pulse-periodic mode where overheating of the separative foil limits the average electron current density, and hence the lasing output power.

Let us note that in the case where the rate of circulation of the laser mixture is inadequate and the limiting pulse recurrence rate depends on the pumping pulse parameters, the mode considered above is non-optimum. However, there are no special technical difficulties involved in ensuring the necessary laser mixture flowrate at which the time required for the gas to cross the discharge gap is much less than the time between pulses. Therefore it is the mode with maximum electron beam utilization factor that is of the greatest practical interest.

In conclusion, the authors are sincerely grateful to A. M. Soroka for useful discussions.

REFERENCES

1. N. G. Basov, I. K. Babayev, V. A. Danilychev, M. D. Mikhaylov, V. K. Orlov, V. V. Savel'yev, V. G. Son, N. V. Cheburkin, KVANTOVAYA ELEKTRONIKA, Vol 6, 1979, p 772.

2. N. A. Blinov, I. A. Leont'yev, V. K. Orlov, N. V. Cheburkin, KVANTOVAYA ELEKTRONIKA, Vol 4, 1977, p 1808.

3. A. F. Suchkov, B. M. Urin, Preprint No 117, Lebedev Physics Institute, Moscow, 1974.

4. A. F. Vitshas, Ye. P. Glotov, V. A. Danilychev, V. N. Orlov, N. V. Cheburkin, V. V. Chulkov, Preprint No 192, Lebedev Physics Institute, Moscow, 1979.

5. A. N. Lobanov, V. K. Orlov, A. F. Suchkov, V. M. Urin, Preprint No 199, Lebedev Physics Institute, Moscow, 1977.

6. N. G. Basov, V. A. Danilychev, A. A. Ionin, I. B. Kovsh, V. A. Sobolev, A. F. Suchkov, B. M. Urin, KVANTOVAYA ELEKTRONIKA, Vol 2, 1975, p 2458.

6610
CSO: 1862

UDC 621.373.826.038.825.4

ENERGY CHARACTERISTICS OF A COPPER VAPOR LASER WITH TRANSVERSE DISCHARGE

Moscow KVANTOVAYA ELEKTRONIKA in Russian Vol 7 No 9(99) Sep 80 pp 1948-1954 manuscript received 19 Mar 70

[Article by A. Yu. Artem'yev, Yu. A. Babeyko (deceased), O. M. Bakhtin, B. L. Borovich, L. A. Vasil'yev, V. Ye. Gerts, Ye. P. Nalegach, G. Ye. Ratnikov, L. V. Tatarintsev and A. N. Ul'yanov]

[Text] An investigation is made of the major energy characteristics of a copper vapor laser with transverse discharge. Relations are found for the average lasing power on the yellow and green emission components as dependent on the amplitude and recurrence rate of the excitation pulses, the discharge chamber wall temperature and the buffer gas pressure. Results of a study of the current-voltage characteristics of the discharge are given. An average emission power of 75 W is attained at a pulse recurrence rate of 3 kHz.

To excite molecular gas-discharge lasers (for example lasers based on CO_2, N_2 and so on), various transverse electric discharge arrangements have been used that have increased the specific and output parameters of these lasers. However, until now this type of discharge has almost never been used for exciting metal vapor lasers. This is due primarily to the technological difficulties of producing a high-temperature laser chamber (~2000 K), and secondarily to the necessity of developing a generator that produces nanosecond pulses of high voltage with sufficiently low wave impedance to get the required current density. Therefore the transverse excitation scheme so far has been used only in chambers with small useful volume [Ref. 1, 2] or for excitation of copper halides [Ref. 3, 4] with a working temperature range of about 900 K, which is considerably lower than for pure metals.

This paper gives the results of studies of the energy characteristics of a copper vapor laser with transverse excitation. The discharge gap of the chamber was formed by two sectionalized electrodes. The temperature inside the chamber was controlled up to 2000 K by special heaters with power supply from a low-voltage source. The electrode system, heaters, high-voltage insulation and thermal insulation were installed inside a water-cooled metal chamber.

Excitation of the high-voltage nanosecond discharge was by pulse voltage generator with the output stage connected in a Blümlein circuit, and consisted of resonant charging cable shaping lines and thyratron commutators. A step-down cable transformer was used to match the pulse voltage generator to the discharge gap.

The optical cavity was formed by a flat dielectric mirror with reflectivity of 99% for green and yellow emission components ($\lambda_1 = 510.6$ nm and $\lambda_2 = 578.2$ nm) and a plane-parallel plate.

The amplitude and shape of the excitation pulses on each section of the discharge gap were measured by corresponding sensors: a pulse transformer (for voltage U) and a Rogowski loop (for current J). Registration was by 6LOR-04 oscilloscopes. Transient recovery times for the measurement channel were 10 ns for voltage and 20 ns for current. Voltage pulse duration was $\tau \sim 100$ ns, and the rise time of the voltage pulse was ~60 ns.

The equivalent circuit of the discharge system in the chamber can be represented as a series-connected RL network, where R is the ohmic resistance of the discharge plasma, and L is the inductance of the current-carrying leads and the discharge gap itself (estimates show that capacitive currents are negligible). Direct measurements of inductance as well as oscillograms of the pulses of current and voltage $\left(L = \left(U \Big/ \frac{dJ}{dt} \right)\Big|_{J=0} \right)$ gave $L \approx 60$ nH. In order to study the current-voltage and energy characteristics of the discharge, it is necessary to convert from the measured value of the voltage pulse U to the resistive component of this pulse $U_R = U - LdJ/dt$.

Visual inspection showed that the discharge fills the entire discharge gap uniformly. Sometimes the formation of "strands" or "arcs" is observed. Strong arcing is accompanied by an abrupt reduction in output parameters of the laser. Experiments show that with degassing of the chamber to such an extent that a static vacuum on a level of $\sim 10^{-3}$ mm Hg is retained at working temperatures for several minutes, almost no arcing is observed at neon pressures right up to 1-2 atmospheres. It should also be noted that the probability of arcing increases with increasing amplitude and recurrence rate of the excitation pulses.

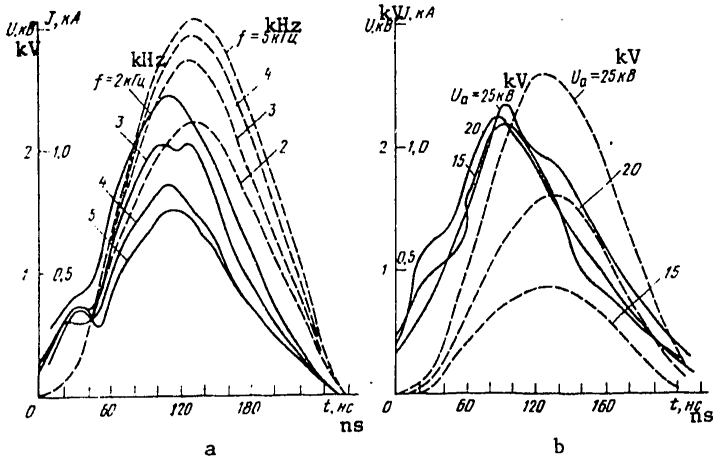

Fig. 1. Shape of current pulses (dotted lines) and voltage pulses (solid lines) at a neon pressure of 0.7 atmosphere and constant $U_a = 25$ kV (a) and $f = 3$ kHz (b)

Fig. 1 shows current pulses and the resistive components of voltage pulses across the discharge gap with changing recurrence rate f and amplitude U_a of the voltage on the thyratron anode. A characteristic feature of the current-voltage curves is a reduction in the resistive component of voltage across the gap with simultaneous increase in current as the pulse recurrence rate increases. With increasing amplitude of the pulses on the thyratron anode, there is almost no change in the resistive component of the voltage pulse across the discharge gap, and only the amplitude of the current pulses increases. This is an important feature of the investigated system since it is a considerable limitation on the capabilities for varying the electric field strength in the discharge gap. Let us also note that a reduction of buffer gas pressure and increase in copper concentration (wall temperature in the discharge zone) leads to a reduction in the resistive component of voltage across the gap and an increase in discharge current.

Matching between the pulse voltage generator and the discharge gap with respect to energy input is fairly satisfactory. About 70% of the power that the pulse voltage generator can provide to a matched ohmic load (at $U_a = 25$ kV, $f = 3$ kHz) is released in the discharge. Under these conditions the pulse energy is weakly dependent on the pulse recurrence rate.

The above-mentioned peculiarities of the current-voltage characteristics of the discharge can be interpreted as follows. The resistive component of the voltage across the discharge gap depends on the amplitude of the voltage generator output pulse and the ratio of the ohmic R and inductive $\sim\pi L/\tau$ components of the discharge and the wave impedance ρ of the cable transformer. The lower R is as compared with $\pi L/\tau$ and ρ, the lower will be the resistive component of the voltage across the discharge gap. The resistance of the discharge is

$$R \sim N/n_e, \tag{1}$$

where N is the concentration of Ne atoms.

Electron concentration n_e is determined by processes of ionization of copper and neon during the discharge and recombination of the plasma in the intervals between pulses. Based on the equation for plasma recombination

$$dn_e/dt = -k_p n_e^3, \tag{2}$$

which accounts only for the fastest process under our conditions [Ref. 5] (k_p is rate constant of ternary recombination), we can easily find that the initial concentration of electrons for discharge development is

$$n_e^{(0)} \approx (f/2k_p)^{1/2}. \tag{3}$$

Substituting $f = 3 \cdot 10^3$ s^{-1} and $k_p = 10^{-23}$ cm^6/s^{-1} [Ref. 5] in (3), we get $n_e^{(0)} \approx 10^{13}$ cm^{-3}, which is several orders of magnitude greater than the thermal concentration of electrons. Thus the conditions for discharge development differ considerably for the pulse-periodic mode and the isolated pulse mode. In the pulse-periodic mode the plasma does not have time to fully recombine in the intervals between pulses, and the discharge develops through the conductive gas, i. e. there is an analogy with discharge when the gas is pre-ionized by an electron beam or ionizing radiation. In this case an increase in pulse recurrence rate leads to

an increase in initial electron concentration, and consequently to a reduction in discharge resistance, which explains the nature of the dependence of current-voltage characteristics on f.

The discharge resistance is also determined by the rates of processes of ionization of copper and neon atoms, which depend on the average electron energy ε. For discharge in a Cu-Ne mixture, electron energy was calculated in Ref. 6, where it is shown that ε is mainly a function of the parameter $E/\sqrt{Nn}$ (E is electric field strength, n is copper atom concentration). By using the results of calculations of Ref. 6 and the current-voltage curves, and disregarding the potential drop near the electrode, we can evaluate concentration n_e and electron energy. Under optimum conditions (with respect to lasing), we have at the maximum $n_e \approx 10^{13}$ cm^{-3}, $\varepsilon = 5$-7 eV. In this case we have direct ionization of copper atoms ($k_1 \approx 10^{-8}$ cm^3/s at $\varepsilon = 7$ eV [Ref. 6]), and apparently two-stage ionization of neon atoms via resonant and metastable levels (direct ionization of neon is negligible).

An increase in copper concentration (chamber wall temperature) leads to a reduction of average electron energy, and hence of copper ionization rate. However, an increase in the collision rate between electrons and copper atoms is apparently a stronger factor that increases the number of electrons and reduces discharge resistance.

An increase in recurrence rate and amplitude of the pulse voltage generator output also involves an increase in the average power invested in the discharge, which leads to rising temperature of the gas and chamber walls. Since the discharge region occupies a small space compared with the total volume of the chamber, heating of the gas leaves neon pressure in the chamber practically unchanged, but may reduce neon concentration in the discharge gap. Rising wall temperature increases copper concentration. Both effects reduce discharge resistance and may explain why only discharge current rises with increasing pulse voltage amplitude while the voltage across the gap remains practically unchanged.

The emission characteristics of a copper vapor laser with transverse discharge differ considerably from the parameters of a laser with longitudinal discharge. This applies first of all to the way that the average lasing power depends on pulse recurrence rate and on buffer gas pressure. In the investigated laser the region of optimum pressures lies in a range of 0.7-1 atmosphere, and lasing power drops only slightly with rising pressure up to 1.5 atmosphere. At low neon pressures (of the order of 10-30 mm Hg), lasing power is low.

The range of optimum pulse recurrence rates for the pulse voltage generator lies at 2-5 kHz, and depends on pulse amplitude, chamber wall temperature T and the duration τ of the excitation pulse (Fig. 2). An increase in U_a, T and τ leads to a reduction in optimum rate f_{opt}.

Lasing power is strongly dependent on chamber wall temperature, which was measured by a pyrometer and thermocouples. The optimum temperature is 1400°C, the working temperature range is about 200°C, the power of the pulse

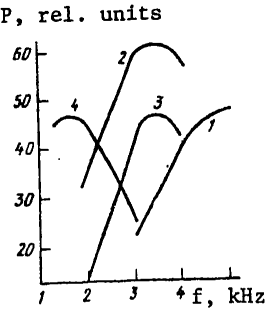

Fig. 2. Average lasing power P integrated with respect to components as a function of f for storage lines with a length L = 4 (*1*), 6.5 (*2*, *3*) and 13 m (*4*) and U_a = 15 (*3*) and 20 kV (*1*, *2*, *4*)

voltage generator released in the discharge leads to additional heating of the walls by approximately 50-100°C.

Under optimum conditions (with respect to f and T) the laser operates on two spectral components ($\lambda_1 = 510.6$ nm and $\lambda_2 = 578.2$ nm) with about the same power. As f or T is increased beyond the optimum, the lasing power of the green component first begins to decrease, and this fall-off is not uniform over the beam cross section. Lasing first stops on this component in the center of the discharge gap, and the near-field pattern shows a horizontal yellow band (under optimum conditions the near-field pattern is in the form of a rectangle with the shadow of the electrodes uniformly lit by green light since the sensitivity of the eye in this region is considerably higher than in the yellow region of the spectrum). As f or T increases, the yellow band expands, and then lasing stops on the yellow component as well, becomes concentrated in the regions near the electrodes and finally stops altogether.

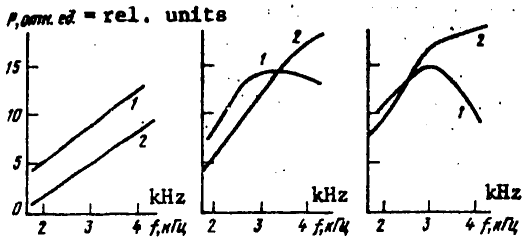

Fig. 3. Average lasing power P as a function of f for λ_1 (*1*) and λ_2 (*2*) at $U_a = 15$ (a), 20 (b) and 25 kV (c); T = 180°C

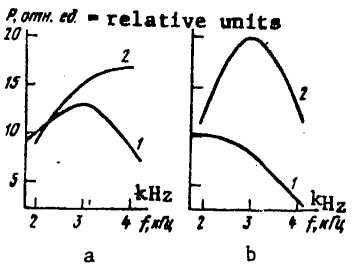

Fig. 4. Average lasing power P as a function of f for λ_1 (*1*) and λ_2 (*2*) at $U_a = 20$ (a) and 25 kV (b); T = 1530°C

Fig. 3 and 4 show how the average lasing power of the individual components depends on U_a, f and T. We can see that lasing on λ_1 reaches saturation sooner and then begins to decline sooner than on λ_2.

When the pulse voltage generator is energized, the chamber walls are additionally heated, and consequently there is an increase of copper concentration in the space of the chamber. As a result, the laser parameters do not settle down for several minutes after energizing the pulse voltage generator. Lasing first starts on the green component, which is also first to reach the maximum. If f or T is greater than the optimum, a drop in power is observed first on the green component, and then on the yellow component as well.

Lasing power increases linearly with an increase in the amplitude of the voltage pulses U_a at the optimum temperature. This is a natural consequence of the fact that as U_a increases it is only the amplitude of the discharge current pulse that rises, while the voltage across the gap remains unchanged. As a result, the

laser efficiency falls off as $1/U_a$ with increasing U_a since the power of the pulse voltage generator increases as U_a^2.

The following maximum output parameters were attained under optimum conditions: average emission power 75 W at recurrence rate f = 3 kHz, efficiency with respect to pulse voltage generator power across a matched load 1.6%. Under these conditions the neon pressure was about 0.7 atmosphere, chamber wall temperature ~1400°C.

The major features of the radiation characteristics can be interpreted as follows. For effective laser operation it is necessary that the average electron energy should lie in a range of 4-7 eV. At lower energy there is a reduction in the difference between the rates of population of upper and lower laser levels by electron impact [Ref. 7]. The critical electron energy at which these rates become equal is 2-3 eV. At higher energy there is an increase in the fraction of losses to ionization and excitation of high levels of copper and neon atoms. The electron energy is determined by electric field strength and by the concentration of copper and neon atoms (the parameter $E/\sqrt{Nn}$). The higher N is, the greater will E have to be for the same n. On the other hand, other things being equal, the lasing power is proportional to the electron concentration n_e. In virtue of the fact that the electron drift velocity $v_{dr} \sim 1/N$, greater current density is required at low N to get the same electron concentration as at high N. In the given laser, the discharge cross section is large, and it is difficult to ensure large current density. Therefore the optimum mode is one with high neon pressure, increased electric field strength and low current density. In lasers with longitudinal discharge, where it is difficult to get high electric field strength, the optimum mode is one with low N and high current density [Ref. 8]. Which mode is more advantageous from the standpoint of laser efficiency must be determined by more detailed calculations and experiments.

Various factors may limit the pulse recurrence rate in a laser with transverse idscharge.

1. With increasing pulse recurrence rate there is an increase in the electron concentration and a reduction in discharge resistance. The result is a reduction in electric field strength and a drop in average electron energy. Lasing stops when the pulse recurrence rate reaches a critical value.

2. In the optimum working mode of the laser the temperature of the gas (the heavy particles) in the center of the gap may reach ~3000 K as shown by thermophysical calculations. Thermal population of the lower laser level becomes appreciable at such a temperature. The lower laser level may also be populated by electron impact if the electrons do not have time to cool off in the interval between pulses.

3. There is a redistribution of particle density in the discharge gap due to heating of the gas. The neon and copper concentration in the center of the gap is less than near the electrodes. As a result there is a change in plasma resistivity with respect to the height of the gap and both a general reduction of discharge resistance with associated drop in electric field strength, and a redistribution of the field along the gap, the field being minimum in the center of the gap. Apparently it is this circumstance that is responsible for lasing disruption in the horizontal band in the center of the gap with increasing pulse recurrence rate or copper concentration.

The difference in behavior of the green and yellow emission components can be attributed to the fact that the lower laser level for the yellow component is 2000 cm^{-1} higher than for the green. Therefore thermal effects begin to show up later on the yellow component. In addition, the critical electron energy for the yellow component is apparently lower than for the green.

At present it is not possible to precisely define the relative role of each of the above-mentioned effects in limitation of pulse recurrence rate. Most probably we are dealing with the composite action of these effects.

The way that lasing power depends on wall temperature is apparently determined by two parameters: the concentration of copper atoms and the average electron energy. At low temperatures ($\leq$1400°C) the concentration of copper atoms is low, and as temperature increases there is a reduction in average electron energy (the parameter $E/\sqrt{Nn}$ decreases) approaching the critical energy. When the pulse voltage generator is energized the chamber walls are additionally heated (~100°C) and over a period of several minutes there is an increase of copper concentration in the discharge gap. If we assume that the critical electron energy for the yellow component is lower than for the green, then lasing cutoff on the yellow component should occur later than on the green, and this is what is observed in the experiment.

Our research showed that with respect to working conditions a copper vapor laser with transverse discharge differs considerably from a laser with longitudinal discharge, which makes it necessary not only to match the output impedance of the pulse voltage generator to the resistance of the discharge gap, but to ensure formation of a plasma with required characteristics as regards the concentration and energy of electrons. Besides, an increase in the power invested in the discharge leads to an increase in the influence that thermal effects have on radiation parameters. Using pulse voltage generators with relatively high recurrence rate increased the emission pulse energy by more than an order of magnitude over the best results achieved heretofore [Ref. 8].

In conclusion the authors thank E. I. Molodykh, S. A. Negashev, G. N. Nikolayev, V. M. Rybin, V. M. Ryazanskiy and A. V. Timoshenko for useful discussion.

REFERENCES

1. V. S. Aleksandrov, Yu. A. Babeyko, A. A. Babayev, O. I. Buzhinskiy, L. A. Vasil'yev, A. V. Yefimov, S. I. Krysanov, G. N. Nikolayev, A. A. Slivitskiy, A. V. Sokolov, L. V. Tatarintsev, V. S. Tereshchenkov, KVANTOVAYA ELEKTRONIKA, Vol 2, 1975, p 2077.

2. P. A. Bokhan, V. B. Shcheglov, KVANTOVAYA ELEKTRONIKA, Vol 5, 1978, p 381.

3. G. V. Abrosimov, V. V. Vasil'tsev, KVANTOVAYA ELEKTRONIKA, Vol 4, 1977, p 909.

4. P. James, IEEE J, QE-14, 1978, p 405.

5. Ya. B. Zel'dovich, Yu. P. Rayzer, "Fizika udarnykh voln i vysokotemperaturnykh gidrodinamicheskikh yavleniy" [Physics of Shock Waves and High-Temperature Hydrodynamic Phenomena], Moscow, Nauka, 1968.

6. A. Kh. Mnatsakanyan, G. V. Naydin, N. P. Shternov, KVANTOVAYA ELEKTRONIKA, Vol 3, 1978, p 597.

7. D. A. Leonard, IEEE J, QE-3, 1967, p 380.

8. A. A. Isayev, G. Yu. Lemmerman, KVANTOVAYA ELEKTRONIKA, Vol 4, 1977, p 1413.

6610
CSO: 1862

UDC 621.378+629.7.036.5

CONCERNING THE POSSIBILITY OF USING GASDYNAMIC PYROLYSIS FOR PRODUCING LASING MEDIA

Moscow KVANTOVAYA ELEKTRONIKA in Russian Vol 7,No 10(100), Oct 80 pp 2221-2224 manuscript received 3 Mar 80

[Article by A. S. Biryukov, V. M. Marchenko and A. M. Prokhorov, Physics Institute imeni P. N. Lebedev, USSR Academy of Sciences, Moscow]

[Text] An examination is made of the feasibility of using a method of gasdynamic pyrolysis of substances with reserve internal chemical energy in heterogeneous mixing of gas streams to produce lasing media.

Practical application of gasdynamic lasers depends on increasing the specific energy output and the capability of working in an open cycle, i. e. with discharge of spent gases into the ambient atmosphere. Powerful gasdynamic lasers, like chemical lasers, use exothermal chemical reactions as the source of energy. The energy of the reactions is expended on producing active media and a gasdynamic flow, and therefore efforts should be aimed at optimizing the ratio between the energy fluxes in both channels.

From the kinetics of formation of inverse populations of levels we find that the greatest specific energy reserves in the active media of gasdynamic CO_2 lasers are attained in models of instantaneous mixing ($\tau_m \leqslant \tau_r$) of supersonic flows of the donor (N_2) and the acceptor (CO_2) gases [Ref. 1]. The relaxation time of upper lasing levels $\tau_r \gtrsim 0.1$ ms is usually greater than the time of passage of the medium through the laser cavity. The characteristic time of diffusion mixing [Ref. 1] $\tau_m = \kappa F/D$ (F is the cross sectional area of the mixing jets; κ is a factor that characterizes the degree of intermixing; D is the coefficient of laminar or turbulent diffusion) can be shortened by reducing the cross section of the jets and by turbulizing their boundaries. It is for this reason that efforts are made to reduce the nozzle dimensions in gas jet mixing systems. Making jet mixing systems with transverse dimension $d \approx 5$ mm in large-volume continuous-action facilities by using arrays of miniature nozzles [Ref. 2, 3] is a complicated technical problem. Gasdynamic perturbations on the boundaries of the jets lead to heating of the gas stream [Ref. 4] and losses to relaxation.

A further step in the direction of reducing τ_m is heterogeneous mixing of gas flows, including flows of chemically reacting components, as proposed in Ref. 4-6. In heterogeneous mixing a stream of aerosol particles measuring about 10 μm is directed into a shaped homogeneous flow of gas mixture with a predetermined chemical makeup

and thermodynamic parameters. The particles penetrate deeply into the mixture and are converted to gas as a result of aerodynamic heating. The time of molecular mixing in the wakes of the particles may be reduced by a factor of more than 100 as compared with gas jet mixing. Gasdynamic flow perturbations are also considerably reduced. The use of heterogeneous mixing can appreciably improve the energy characteristics of a CO_2 gasdynamic laser and enables discharge of spent gases into the atmosphere. The difficulties of realizing such systems lie in the necessity for developing fuels with combustion temperature of the order of 4000 K containing products with a minimum content of quenching impurities [Ref. 3].

Ref. 7 discusses the possibility of an increase in working pressures in chemical lasers as a result of laser pyrolysis in a mixture of fuel and oxidant. The reaction of thermal dissociation of NaN_3 is given as an example, where atomic Na is given off that is capable of initiating a reaction of hydrogen with halides at ordinary temperatures.

In this paper we consider a method of producing a stream of active medium based on gasdynamic pyrolysis of aerosol particles of substances with reserve internal chemical energy. This method enables improvement of the energy characteristics of gasdynamic lasers through nonequilibrium chemical reactions. If a stream of particles of such an aerosol is directed into a high-enthalpy subsonic or supersonic gas flow, the particles will be heated by gasdynamic interaction to the temperature of chemical dissociation. Part of the internal energy of the initial substance will be carried off by the products of dissociation, which may be in chemical and thermal nonequilibrium. Thus the problem is to ensure thermodynamic conditions conducive to chemical reactions and relaxation processes in the flow such that there is a buildup of the donor gas that is the carrier of thermally nonequilibrium excitation.

Let us examine the feasibility of realizing the method as exemplified by gasdynamic pyrolysis of NaN_3 aerosol particles introduced into a flow of gas mixture containing molecules of N_2, CO and CO_2.

It is shown in Ref. 8 that thermal dissociation of sodium azide produces N_3 radicals with density in the flow reaching 10^{13} cm^{-3}. The rate constant of dissociation of NaN_3 powders in $g/cm^2 \cdot s$ depends on the specific surface S of the particles and is very strongly dependent on temperature of the process [Ref. 13]. In accordance with Ref. 8 we will assume that thermal dissociation of sodium azide leads to production of electronically excited molecules of N_2 ($^3\Sigma_u^+$) in the reaction

$$2N_3 \rightarrow N_2(^3\Sigma_u^+) + 2N_2(^1\Sigma_g^+). \quad (1)$$

We will disregard the probable vibrational excitation of products in this reaction. The further evolution of excitation in the system is quite fully described by the following elementary processes:

$$N_2(^3\Sigma_u^+) + N_2(^1\Sigma_g^+) \rightarrow 2N_2^*(^1\Sigma_g^+), \quad (2)$$

$$+CO(^1\Sigma^+) \rightarrow N_2(^1\Sigma_g^+) + CO(^3\Pi), \quad (3)$$

$$\rightarrow N^*_2(^1\Sigma_g^+) + CO^*(^1\Sigma^+), \quad (4)$$

$$N_2(^3\Sigma_u^+) + CO_2(^1\Sigma_g^+) \rightarrow , \quad (5)$$

$$CO(^3\Pi) + CO(^1\Sigma^+) \rightarrow 2CO^*(^1\Sigma^+), \quad (6)$$

$$+ N_2(^1\Sigma_g^+) \rightarrow CO^*(^1\Sigma^+) + N_2^*(^1\Sigma_g^+) , \quad (7)$$

$$+CO_2(^1\Sigma_g^+) \rightarrow . \quad (8)$$

(1) Константа скорости	(2) Значение константы, см³/с	(3) Литература
K_1	$5\cdot10^{-12}$	[8]
K_2	$<7\cdot10^{-15}$	[9]
K_3+K_4	$(0,18—4,6)\cdot10^{-11}$	[10]
K_3	$\sim(K_3+K_4)$	[11]
K_5	10^{-14}	[9]
K_6	$(0,76—2,8)\cdot10^{-10}$	[9, 11]
K_7	$(0,7—1,5)\cdot10^{-11}$	[11]
K_8	$(1,2—2,0)\cdot10^{-11}$	[9, 11]

KEY: 1--Rate constant
2--Value of the constant, cm^3/s
3--Reference

Radiative decay of metastable states of $N_2(^3\Sigma_u^+)$ and $CO(^3\Pi)$ can be disregarded in comparison with collisional decay. The rate constants of processes (1)-(8) are summarized in the table.

From the standpoint of conversion of the energy released in pyrolysis of sodium azide to vibrational degrees of freedom of the donor gas $CO^*(^1\Sigma^+)+N^*(^1\Sigma_g^+)$, the useful processes are (1)-(4), (6) and (7). The state of the products of reactions (5) and (8) is unknown; however, the table shows that process (5) can be disregarded as compared with (3) and (4), while process (8) can be disregarded in comparison with (6) if $[CO]\gtrsim[CO_2]$.

In processes of relaxation of the state $N_2(^3\Sigma_u^+)$ as shown in (2)-(8), n vibrational quanta of donor gas are produced. Since up to 96% of the energy of $CO(^3\Pi)$ in process (6) goes to vibrational degrees of freedom [Ref. 12], $n\approx 20$. Nearly all the energy of the excited electron states is converted to vibrational energy of the donor gas if the concentration $[N_3]\gtrsim(K_1\tau_r)^{-1}\approx 2\cdot10^{15}$ cm^{-3}.

Processes (3), (6) and (7) are so fast that $[N_2(^3\Sigma_u^+)]$ and $[CO(^3\Pi)]$ are quasisteady. Therefore the average number of vibrational quanta $\Delta\varepsilon$ accumulated in the process of pyrolysis of spherical NaN_3 particles with initial radius r_0 is found by sequential integration of the system of equations

$$\frac{d[N_3]}{dt}=3a\frac{N_д}{\mu}\frac{\mu_д K}{\rho r_0}\left(1-\frac{K}{\rho r_0}t\right)^2-2K_1[N_3]^2;$$

$$\frac{d(\Delta\varepsilon)}{dt}=\frac{nK_1[N_3]^2}{N_д}$$

where a is the mass fraction of solid phase with density ρ; $N_д$ is the concentration of donor gas molecules; $\mu_д$, μ are the masses of the molecules of donor gas and NaN_3. In the case of slow dissociation of particles on a time interval $\tau_r<<K/(\rho r_0)$, the solution of the system takes the form

$$\Delta\varepsilon=|A|\left(t-\frac{2}{\alpha}\frac{e^{\alpha}-1}{e^{\alpha t}+1}\right), \qquad (9)$$

where

$$A=\frac{3an\mu_д K}{2\mu\rho r_0};\ \alpha=\left(\frac{24a\mu_д N_д K_1 K}{\mu\rho r_0}\right)^{1/2}.$$

The average number of vibrational quanta per molecule of donor gas $\varepsilon_V=(\exp\theta/T_V-1)^{-1}$ is of the order of 0.2 in conventional CO_2 gasdynamic lasers for "congealing" temperatures $T_V = 1800$ K (θ is the characteristic temperature of vibrations). Let us evaluate the constant K where pyrolysis of sodium azide particles at $\alpha = 0.1$ and $N_Д = 10^{18}$ cm^{-3} results in a buildup of $\Delta\varepsilon = \varepsilon_V$ in time $\tau_Г = 0.1$ ms. Calculation by (9) at $r_0 = 1$ μm gives $K = 0.33$ $g/cm^2 \cdot s$. Such a rate of particle dissociation will double the vibrational energy density in the flow of the CO_2 gasdynamic laser. This value of K is 1000 times as high as that measured at T = 633 K [Ref. 13], and may be reached by extrapolation of K(T) at $T \approx 650$ K. The estimate is based on the assumption that the main channel of dissociation of NaN_3 is generation of N_3 radicals. If other channels of dissociation exist, there is still a high probability that the liberated energy will go to vibrational degrees of freedom of the donor gas.

Heating of particles to $T \approx 650$ K is ensured when they are injected into the flow either in the critical section of the nozzle or in the supersonic part [Ref. 5, 6]. Where necessary, heating time is reduced by preheating the particles right up to the liquid phase [Ref. 14]. The induction time of thermal dissociation of sodium azide decreases with rising temperature and with a reduction in particle size [Ref. 13]; however, this factor has not been completely quantitatively analyzed, and it may turn out to be longer than the characteristic gasdynamic times of 10-100 μs. To attain the highest rate of dissociation, injection of the particles into the flow must be delayed by a time close to the induction period.

The specific energy reserve of the mixture after pyrolysis of NaN_3 is estimated by the relation

$$W = h\nu \frac{(N_Д/N_c)(\varepsilon_v + \Delta\varepsilon) - \varepsilon_2(T)}{(N_Д/N_c)\mu_Д + \mu_c},$$

where hν is the energy of a quantum of CO_2 laser radiation; N_c is the concentration of CO_2 molecules; μ_c is the mass of CO_2 molecules; $\varepsilon_2(T)$ is the fraction of CO_2 molecules on the lower working level. At $N_c/N_Д = 0.1$, $W \approx 150$ J/g.

We get a gas flow temperature of the order of 650 K both with the reduced expansion in the nozzle assembly, and due to part of the internal (chemical) energy that is transferred to translational degrees of freedom. A rise in T relaxes the conditions for expelling spent gases into the ambient atmosphere as a consequence of the pressure increase ($N_Д$ = const).

As applied to development of lasers using gasdynamic pyrolysis, sodium azide is not a complete success because of the relatively low rate of thermal dissociation in the presence of atomic sodium in the products, which may lead to additional losses. Substances for which dissociation takes place more rapidly will be more suitable for this purpose, the dissociation being into molecular gases [Ref. 14] with nonequilibrium internal energy. As in conventional gasdynamic lasers, the lower level is cleaned by H_2O molecules present in small amounts in the main flow.

In principle, heterogeneous mixing can be used to increase the working pressures in chemical lasers as well; however, in this case it is more complicated to ensure a pumping rate of the working component or donor gas that appreciably exceeds its relaxation rate (for example in HF lasers).

Thus heterogeneous mixing of gas fluxes not only improves existing laser designs, but also leads to new designs as well as expanding the class of usable substances.

REFERENCES

1. S. A. Losev, "Gazodinamicheskiye lazery" [Gasdynamic Lasers], Moscow, Nauka, 1977.

2. B. A. Vyskubenko, Ye. T. Demenyuk, G. A. Kirillov, Yu. V. Kolobyanin, S. B. Kormer, N. A. Nitochkin, DOKLADY AKADEMII NAUK SSSR, Vol 248, 1979, p 81

3. P. E. Cassady, A. L. Pindroh, J. E. Newton, AIAA J., Vol 17, 1979, p 845.

4. A. S. Biryukov, V. M. Marchenko, A. M. Prokhorov, ZHURNAL EKSPERIMENTAL'NOY I TEORETICHESKOY FIZIKI, Vol 71, 1976, p 1726; Preprint Lebdev Physics Institute, No 64, 1976.

5. V. I. Alferov, A. S. Biryukov, Ye. A. Bozhkova, L. M. Dmitriyev, V. M. Marchenko, A. M. Prokhorov, KVANTOVAYA ELEKTRONIKA, Vol 6, 1979, p 1746; Preprint Lebedev Physics Institute, No 275, 1978.

6. V. I. Alferov, A. S. Biryukov, L. M. Dmitriyev, Yu. Ye. Markachev, V. M. Marchenko, A. M. Prokhorov, DOKLADY AKADEMII NAUK SSSR, Vol 248, 1979, p 1093.

7. H. Y. Chiu, R. M. Somers, R. C. Benson, CHEM. PHYS. LETTS, Vol 61, 1979, p 203.

8. L. G. Piper, R. H. Krech, R. L. Taylor, J. CHEM. PHYS., Vol 7, 1979, p 2099.

9. B. M. Smirnov, "Iony i vozbuzhdennyye atomy v plazme" [Ions and Excited Atoms in Plasma], Moscow, Atomizdat, 1974.

10. J. W. Dreyer, D. Perner, C. R. Roy, J. CHEM. PHYS., Vol 61, 1974, p 3164.

11. G. W. Taylor, D. W. Setser, J. CHEM. PHYS., Vol 58, 1973, p 4840.

12. T. G. Slanger, G. Black, J. Fournier, J. PHOTOCHEM., Vol 4, 1975, p 329.

13. R. F. Walker, J. PHYS. CHEM. SOLIDS, Vol 29, 1968, p 985.

14. L. I. Bagal, "Khimiya i tekhnologiya initsiiruyushchikh vzryvchatykh veshchestv" [Chemistry and Technology of Initiating Explosives], Moscow, Mashinostroyeniye, 1975.

[14-6610]

6610
CSO: 1862

UDC 621.378.33

EXPERIMENTAL STUDY OF THE POSSIBILITY OF EFFECTIVELY COUPLING THE ENERGY OUT OF THE ACTIVE MEDIUM OF A DF-CO_2 AMPLIFIER OF NANOSECOND RADIATION PULSES

Moscow KVANTOVAYA ELEKTRONIKA in Russian Vol 7, No 10(100), Oct 80 pp 2240-2243 manuscript received 14 Apr 80

[Article by A. S. Bashkin, N. P. Vagin, S. N. Gerasimov, A. N. Orayevskiy, O. Ye. Porodinkov and M. I. Prishchepa, Physics Institute imeni P. N. Lebedev, USSR Academy of Sciences, Moscow]

[Text] The paper gives the results of an experimental study of a chemical DF-CO_2 amplifier of short pulses with flashlamp initiation working under conditions close to rotational equilibrium on mixtures of $D_2:F_2:CO_2 = 1:3:8$ and 3:3:14 at a total pressure of 0.2-0.75 atmosphere. In operation of the DF-CO_2 amplifier on a mixture of $D_2:F_2:CO_2 = 3:3:14$ (total pressure 0.75 atmosphere) a specific energy output of 11.5 mJ/cm^3 was attained with efficiency relative to the energy invested in the working mixture of about 660%.

It was first suggested in 1977 that a chemical DF-CO_2 amplifier be used to get powerful nanosecond emission pulses [Ref. 1]. The results of that research showed that at atmospheric pressure of a mixture of $D_2:F_2:CO_2:He = 1:1:4:5$ with emission pulse duration of $\tau_i \sim 3$ ns the specific energy output may be 5-12 mJ/cm^3 at an initiation level of $(5\text{-}15)\cdot 10^{15}$ cm^{-3}. The technical efficiency for the case of optical initiation under these conditions may reach $\eta_t \sim 15\%$ assuming total interception of the radiation of a source of photoinitiation that has an efficiency of ~5%. Such high theoretical values of specific energy output and technical efficiency have stimulated interest in experimental research into the possibilities for effectively coupling the energy out of the working medium of a DF-CO_2 amplifier of nanosecond radiation pulses.

The experimental facility shown in Fig. 1 was used for doing the studies. The facility consisted of two principal parts: a master laser and a chemical DF-CO_2 amplifier. The master was a TE-CO_2 nanosecond pulse laser with mode-locked operation by injection of a short pulse into the cavity with the required duration on the lasing threshold [Ref. 2]. The TE-CO_2 laser used a working mixture of $CO_2:N_2:He = 2:1:6$ at a pressure of 0.4 atmosphere. The length of the active region was 80 cm, and the cross section was 20 cm^2. The laser cavity was formed by copper mirror M1 plated with gold and with radius of curvature of 47 m, and flat dielectric mirror ЗД2 with 40% reflection. The length of the cavity was 21 m, and determined the time spacing between emission pulses in the train at the output of the

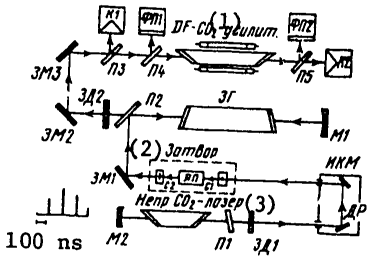

a b

Fig. 1. Typical appearance of pulse train at the output of the master laser (a) and diagram of the experimental facility (b): M1, M2--gold-plated mirrors with nearly 100% reflection; ЗГ--master laser; П1-П5--plane-parallel NaCl plates; ЗД1, ЗД2--dielectric mirrors with reflectivity of 40%; ИКМ--monochromator; C1, C2--polarizers; ЯП--Pockels cell; ЗМ1-ЗМ3--metal mirrors; K1, K2--calorimeters; ФП1, ФП2--photoelectric pickups; ДР--diffraction grating with 100 lines/mm.

KEY: 1--DF-CO_2 amplifier
2--shutter
3--cw CO_2 laser

master laser -- 140 ns. The typical appearance of a pulse train is shown in Fig. 1*a*. The duration of an individual pulse was determined by the duration of the signal injected into the cavity, and was 4 ns at half amplitude. The injected signal was "cut out" from the cw radiation of a CO_2 laser by an electro-optical shutter consisting of a Pockels cell ЯП based on a gallium arsenide crystal placed between crossed polaroids. The polarizer C1 and analyzer C2 were stacks of germanium plates set at the Brewster angle to the optical axis. The radiation pulse was injected into the laser cavity of the master laser through NaCl plate П2. Fabry-Perot etalon П1 in the cavity of the cw CO_2 laser ensured lasing on the single line P(20) of the 10.6 μm band.

The chemical DF-CO_2 amplifier was a quartz tube 100 cm long with inside diameter of 16 mm. The windows were made of NaCl and fastened in stainless steel holders at the Brewster angle to the optical axis. Initiation of the chemical reaction was by two IFP-20 000 flashlamps placed alongside the quartz cell. Foil wrapped around the cell with the lamps acted as a reflector. For an energy $E_i \sim 3$ kJ stored in the capacitor bank, the duration of the initiating pulse was ~5 μs at half height. The length of the discharge gap in the flashlamps was 55 cm, which determined the length of the active region of the chemical amplifier. The aperture of the input and output radiation was measured to determine the active volume of the amplifier. The active volume measured in this way was 46 cm^3.

The amplifier and master laser were synchronized by a G5-15 generator and an ignition unit. The recording equipment included devices for measuring the emission energy characteristics: type PTI and RTE calorimeters, type FPU photoelectric pickups, and also S1-11, IS-7 and S8-7A oscilloscopes.

Experiments were done with mixtures of $D_2:F_2:CO_2 = 3:3:14$ and 1:3:8. Stability of the mixtures during admission was ensured by adding oxygen ($F_2/O_2 = 20$) in such an

amount as not to have any appreciable detrimental effect on the characteristics of the chemical laser [Ref. 3]. The reagent ratio $D_2:F_2 = 1:1$ was selected in accordance with Ref. 1, and the ratio $D_2:F_2 = 1:3$ is typical of hydrogen fluoride chemical lasers [Ref. 3]. Helium was left out of the investigated mixtures since under the conditions of our experiment ($\tau_i \approx 4$ ns and $p_\Sigma < 1$ atm) it cannot effectively relieve the lower lasing level. As implied by Ref. 4, under such conditions a more important question is the rate of rotational relaxation, which falls off with increasing relative concentration of helium in mixtures of constant pressure. For example at the same total pressure the rate of rotational relaxation in conventional mixtures containing helium is 1.6 times lower than in the investigated mixtures [Ref. 5]. To ensure operation of the amplifier under ocnditions close to rotational equilibrium with variation of the pressures in the mixtures over a wide range, the duration of the amplified pulse was taken as 4 ns at half amplitude.

To simplify the experiment, a whole train of pulses was sent to the input of the chemical amplifier from the output of the master laser. This pulse train was made up mainly of 5-6 pulses of different intensity. When the master laser cavity length is appropriately chosen, the ratio of the energies of the first two pulses was matched in such a way that the energy of the first pulse at the input of the chemical amplifier was more than an order of magnitude less than the saturating energy E_s under the conditions of the experiment at pressure of the mixture of 0.75 atm, where $E_s \approx 200$ kJ/cm^2 (by estimates made in accordance with Ref. 4). The energy of the second pulse was comparable with the saturating energy, and in this way, conditions were brought about for effectively coupling out the energy by just this pulse. By comparing oscillograms of the pulse trains at the input and output of the DF-CO_2 amplifier when we know the total energy of the train in both cases, we can follow the evolution of each pulse individually and thus determine the energy coupled out by one pulse.

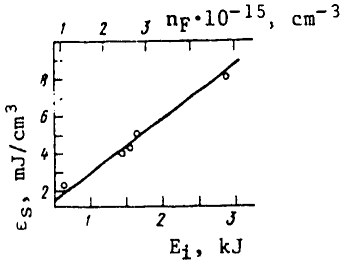

Fig. 2. Specific energy output ε_s as a function of the energy E_i stored in the capacitor bank and initiation level n_F. The relative error of measurement of ε_s is 20%.

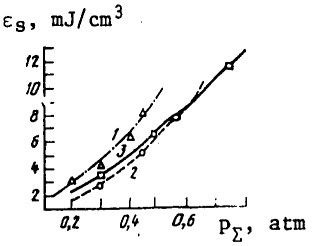

Fig. 3. Dependence of specific energy output ε_s on total pressure p_Σ of working mixtures $D_2:F_2:CO_2 = 1:3:8$ (1, 2) and 3:3:14 (3); $E_i = 3$ (1, 3) and 1.5 kJ (2)

For a mixture of composition $D_2:F_2:CO_2 = 1:3:8$ at pressure of 0.45 atm Fig. 2 shows the way that specific energy output ε_s of a DF-CO_2 amplifier depends on the energy stored in the capacitor bank and on the concentration n_F of active centers produced by the flashlamps by the instant when the energy is coupled out by the short pulse. The concentration was measured by a technique presented in Ref. 6. At the levels of initiation in our experiments this dependence is linear. From this it can be concluded that the efficiency η_f with respect to the energy invested in the working

mixture remains constant. It is defined by the relation $\eta_f = \varepsilon_s(n_F\varepsilon_F)$ where $\varepsilon_F \approx 3.5 \times 10^{-19}$ J is the energy required for formation of a single fluorine atom with optical initiation, and for the data presented on Fig. 2 is equal to 500%. As implied by Fig. 3, for the mixture of the other composition at a pressure of 0.75 atm $\eta_f \approx 660\%$; This value is the maximum in the given experiments (in this case $n_F \approx 5 \cdot 10^{15}$ cm^{-3}).

Fig. 3 shows the way that specific energy output depends on the total pressure of the working mixtures. We can see from this figure that an increase in pressure in all cases leads to a disproportionately fast rise in specific energy output. Such behavior can be attributed to the fact that an increase in pressure causes an increase in the rate of rotational relaxation as well as increasing inversion. Although the specific energy output $\varepsilon_s = 11.5$ mJ/cm^3 reached in our experiments is fairly high, we can expect a further rise with subsequent increase in the total pressure and degree of initiation. From the standpoint of technical efficiency and initiation of large volumes, preference should apparently be given to the mixture $D_2:F_2:CO_2 = 3:3:14$ since the values of η_f and ε_s for this mixture are greater at the same partial pressure of fluorine. In this connection, the maximum chemical efficiency η_{ch} for this mixture is 0.4%, which is lower than for the second mixture, in which $\eta_{ch} \approx 0.9\%$.

The results of Ref. 7 imply that the flashlamps that we used have a luminous efficiency of about 2% for radiation into the absorption band of molecular fluorine. Consequently a chemical DF-CO_2 amplifier of nanosecond pulses operating under conditions of rotational equilibrium may have a technical efficiency of about 13% for the mixtures studied in our research, assuming complete interception of the light of photoinitiation. This is not the limit, since photosources are known with much higher luminous efficiency [Ref. 8].

In conclusion the authors consider it their pleasant duty to thank V. V. Apollonov, E. U. Baykov and N. N. Yuryshev for valuable consultations and useful discussions.

REFERENCES

1. A. S. Bashkin, P. G. Grigor'yev et al., KVANTOVAYA ELEKTRONIKA, Vol 4, 1977, p 1004.

2. P. A. Belanger, J. Boivin, CAN. J. PHYS., Vol 54, 1976, p 720.

3. A. S. Bashkin, V. I. Igoshin, A. I. Nikitin, A. N. Orayevskiy, "Khimicheskiye lazery" [Chemical Lasers], Moscow, VINITI, 1975.

4. G. T. Shappert, APPL. PHYS. LETTS, Vol 23, 1973, p 319.

5. V. A. Danilychev, O. M. Kerimov, I. B. Kovsh, "Molekulyarnyye gazovyye lazery vysokogo davleniya" [High-Pressure Molecular Gas Lasers], Moscow, VINITI, 1977.

6. P. P. Chegodayev, Candidate's dissertation, Affiliate of Physicochemical Scientific Research Institute imeni L. Ya. Karpov, Obninsk, 1974.

7. A. S. Bashkin, N. P. Vagin, O. R. Nazyrov, A. N. Orayevskiy, O. Ye. Porodinkov, N. N. Yuryshev, KVANTOVAYA ELEKTRONIKA, Vol 7, 1980, p 1821.

8. A. F. Aleksandrov, A. A. Rukhadze, USPEKHI FIZICHESKIKH NAUK, Vol 112, 1974, p 193.

6610
CSO: 1862

END